HAL
open science

On the thermo-mechanical theory of field dislocations in transient heterogeneous temperature fields

Manas Vijay Upadhyay

To cite this version:

Manas Vijay Upadhyay. On the thermo-mechanical theory of field dislocations in transient heterogeneous temperature fields. 2020. hal-02439503v4

HAL Id: hal-02439503

https://hal.science/hal-02439503v4

Preprint submitted on 7 Sep 2020

HAL is a multi-disciplinary open access archive for the deposit and dissemination of scientific research documents, whether they are published or not. The documents may come from teaching and research institutions in France or abroad, or from public or private research centers.

L'archive ouverte pluridisciplinaire **HAL**, est destinée au dépôt et à la diffusion de documents scientifiques de niveau recherche, publiés ou non, émanant des établissements d'enseignement et de recherche français ou étrangers, des laboratoires publics ou privés.

On the thermo-mechanical theory of field dislocations in transient heterogeneous temperature fields

Manas V. Upadhyay

Laboratoire de Mécanique des Solides (LMS), Centre National de la Recherche Scientifique (CNRS), Ecole Polytechnique, Institut Polytechnique de Paris, 91128 Palaiseau, France

manas.upadhyay@polytechnique.edu

Abstract

A strong coupling between the field theory of dislocation mechanics and heat conduction is proposed. The novel model, called the thermal field dislocation mechanics (T-FDM) model, is designed to study the dynamics of dislocations during rapid or gradual temperature changes in a body having a heterogeneous temperature distribution; for example, such conditions occur in a heat-affected crystalline solid during an additive manufacturing process. Thermal strains are uniquely separated into compatible and incompatible components via the Stokes-Helmholtz decomposition and the curl of the incompatible part of thermal strains is directly related to the areal dislocation density tensor. A dislocation density evolution (including transport) law is developed and shown to be related to the evolution of the curl of incompatible thermal strains. This relationship demonstrates that dislocation generation, annihilation, motion and/or interactions with other defects can be triggered due to transient temperature changes, and conversely an evolving dislocation density induces temperature changes. The model development is completed with constitutive laws derived from energetic and dissipative considerations. The advantages and consequences of the assumptions of the T-FDM model under rapidly changing temperatures, both spatially and temporally, are discussed. The T-FDM model is intended for application at the length scale where individual dislocations can be characterized. At this level, local thermodynamic equilibrium is found to be a reasonable assumption even for high rates of change of temperature such as those occurring during an additive manufacturing process. Some illustrative examples are presented to demonstrate the applicability of the model and to better understand some of the novel concepts proposed in this work.

Highlights

- Strong temperature gradients during 3D-printing can trigger dislocation dynamics
- A novel fully-coupled dislocation dynamics and heat conduction model is proposed
- The model predicts dislocation dynamics due to temperature changes and vice versa
- Proposed model can deal with high temperature rates during additive manufacturing
- Local thermodynamic equilibrium is respected even under strong temperature rates

Keywords: dislocations, dynamics, thermal stress, constitutive behavior, additive manufacturing

1. Introduction

1.1 Motivation

In this work, we are interested in developing a kinematically and thermodynamically rigorous model to study dislocation mechanics, at the length scale where individual dislocations can be characterized, within a body having a heterogeneous temperature distribution and undergoing rapid and/or gradual temperature changes.

The main motivation for the development of such a model is to enable the study of dislocation structure evolution in a heat-affected crystalline solid during an additive manufacturing (also known as 3D-printing) process. During an additive manufacturing process, just after local deposition due to a moving

heat-source, a liquid material rapidly solidifies within a few milliseconds. Following solidification, as the building continues, the material is subjected to multiple cooling-heating cycles in the solid-state, i.e. solid-state thermal cycling, at varying temperature rates and amplitudes. An illustration of varying temperature rates and amplitudes at a material point during 3D-printing of a metal/alloy wall is shown in Fig. 1. During initial stages of solid-state thermal cycling, temperature amplitudes higher than annealing points and temperature rates of the order of $10^6\ K/s$ can be encountered due to localized heat-matter interactions. Consequently, large transient temperature gradients are formed, which result in strong transient thermal stresses due to internal and/or external constraints. Such rapidly varying temperatures and thermal stresses can result in significant changes in the microstructure, including dislocation structure evolution via dislocation dynamics. During later stages of solid-state thermal cycling, a nearly steady-state heat conduction occurs at relatively high temperatures with respect to room temperature. These relatively high temperatures along with internal stresses due to a metastable microstructure can also result in additional dislocation dynamics, including recovery mechanisms. The existing dislocation dynamics models are unable to handle temperature change driven dislocation dynamics.

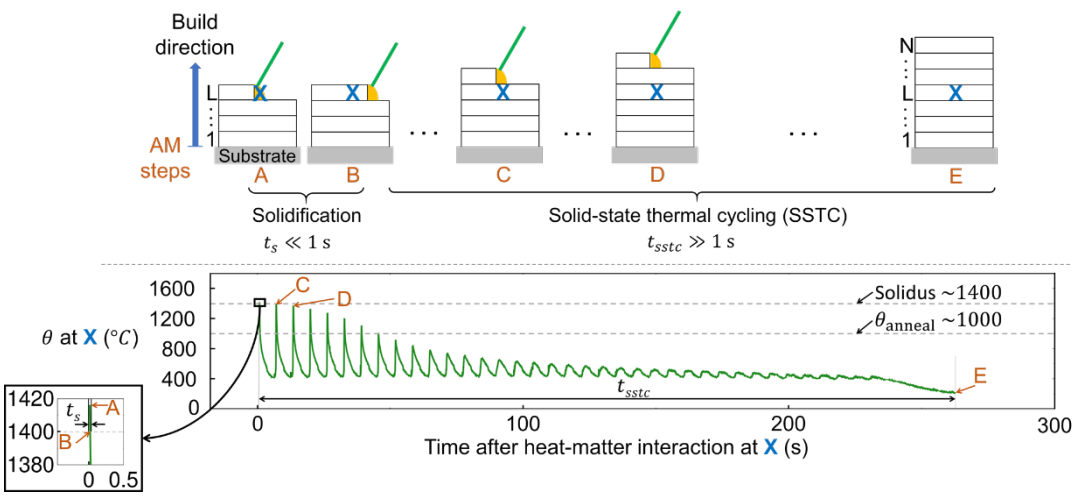

Figure 1: An illustration of temperature (θ) vs time (t) evolution at a material point X during additive manufacturing of a wall. $t = 0$ corresponds to the moment the heat-matter interactions occur at X in a layer L < N, where N is the total number of layers.

1.2 State-of-the-art, aim and structure of the paper

The idea of dislocations being generated from strong temperature gradients was put forth by Kröner (Kröner, 1959, 1958). Kröner noted that in a continuous medium experiencing a heterogeneous temperature field, it is possible to eliminate elastic distortions by introducing dislocations of a density proportional to the curl of thermal strains. An extract from the translated version of (Kröner, 1958) reads, "*Certainly, this process is important when large thermal stresses occur as they do during the cooling of cast iron. Since in this case it is easy to calculate the necessary dislocation arrangement, this is an impressive example of the practical use of the concept that thermal stress is considered as being caused by dislocations.*" This observation by Kröner is also applicable to dislocations formed due to large temperature changes occurring due to solid-state thermal cycling during an additive manufacturing process.

Kröner (Kröner, 1958) argued that a uniform increase in temperature for an unconstrained body results in an increase in the displacement without introducing restoring forces, which is also characteristic of plastic deformation. Based on this postulation, the concept of a quasi-plastic distortion, which does not result in repulsive forces, was introduced. Then, similar to the relationship between an incompatible plastic distortion field and the Nye's tensor (Nye, 1953) in the theory of dislocations, the curl of an incompatible

thermal strain field can be associated with an areal density tensor, which was called the "quasi-dislocation" density tensor (Kröner, 1958). Quasi-dislocations can be induced due to incompatibility in any form of inelastic distortion fields, for example, due to heterogeneous temperatures, magnetic fields, etc. (Kröner, 1958). In this work, the term "thermal quasi-dislocations" is adopted to specifically refer to quasi-dislocations due to incompatible thermal strains. Unlike dislocations, thermal quasi-dislocations do not manifest as line crystal defects in materials; the emphasis is on the mathematical relationship correlating incompatible thermal strains to the areal dislocation density. In (Kröner, 1958), a static theory was proposed for any kind of quasi-dislocations, however, a dynamics model was not developed.

Most existing dislocation dynamics models, both discrete and continuous kind, are designed to study dislocation motion and interactions under isothermal and/or adiabatic conditions. Indeed, there exist couplings between heat conduction and phenomenological elastic-plastic theory (Kratochvil and Dillon, 1969) as well as between heat conduction and dislocation mechanics theory (Acharya, 2011; Acharya and Roy, 2006; Ghoniem et al., 2000; Roy and Acharya, 2006). To the author's knowledge, however, none of the existing dislocation dynamics models account for both incompatible thermal strains due to heterogeneous temperature fields and the relationship between thermal quasi-dislocations and dislocations. For example, in (Kratochvil and Dillon, 1969), scalar parameters were introduced to represent dislocation arrangements of different kinds and phenomenological time evolution laws were proposed. However, due to the phenomenological nature of the evolution laws, it is difficult to connect the modeling approach with crystallography of materials. In (Ghoniem et al., 2000), following thermo-mechanical developments, however, temperature effects were neglected when deriving dislocation driving forces. In (Acharya and Roy, 2006), the role of uniform temperature changes on the mechanical response was considered and in (Roy and Acharya, 2006), the thermal cycling response of a thin-film was studied by simulating uniform temperature changes. Modeling the role of transient temperature gradients on driving dislocation dynamics and vice versa, however, was neither the focus of these works nor was it undertaken there. In (Acharya, 2011), heat conduction was considered in the energetic and dissipation formulations to impose restrictions on the shape of the constitutive relationships for a dislocation mechanics model. The focus of that work was to correlate the specific entropy field as defined in continuum mechanics and the statistical mechanics understanding of entropy, which was then applied to a dislocation mechanics model; an explicit relationship between dislocation density evolution and transient temperature changes was not developed.

Meanwhile, temperature changes induced due to dislocation slip have been studied in a few works. In the earliest works on this topic (Eshelby and Pratt, 1956; Freudenthal and Weiner, 1956), analytical expressions for temperature rise at the level of a slip plane due to the motion of an ensemble of dislocations were proposed. It was concluded that under *normal* slip conditions the temperature rise would correspond to a few degrees to a few tens of degrees; a significant rise in temperature could be achieved due to a sudden release of very closely packed dislocations or at very high loading rates. Dislocation dynamics simulations were performed in (De Hosson et al., 2001) and the simulated temperature changes were compared with analytical solutions for different metals. In all these works, a one way coupling between dislocation dynamics and temperature changes had been proposed, which does not account for dislocation generation, annihilation, motion or interactions with other defects induced by temperature changes.

In this work, a thermodynamically rigorous strongly coupled thermo-elasto-plastic dislocation dynamics model is proposed in a small displacement, small strain and large temperature change framework based on the fundamental idea of thermal quasi-dislocations introduced by Kröner (Kröner, 1959, 1958) and the field dislocation mechanics (FDM) model developed by Acharya (Acharya, 2004, 2003, 2001).

FDM (Acharya, 2004, 2003, 2001) is a thermo-mechanically rigorous model for the dynamics of continuously-represented dislocations. It finds its roots in the elastic theory of continuously distributed dislocations (Bilby et al., 1955; Fox, 1966; Kosevich, 1979; Kröner, 1981, 1958; Mura, 1963; Willis, 1967), which started from the seminal work of Nye (Nye, 1953). Unlike the earlier models that employed the

eigenstrain approach (Eshelby, 1957) to solve the mechanical problem for a dislocation, FDM uses the Stokes-Helmholtz orthogonal decomposition of the elastic/plastic distortion fields into compatible and incompatible components. The curl of the incompatible part of the elastic/plastic distortion is related to the areal dislocation density field, which makes FDM a non-local model. Nevertheless, it does not require using higher-order stresses/higher-order traction boundary conditions, which are typical in gradient plasticity models (for example (Forest, 2008)) or micro-stress/micro-traction conditions (for example, (Gurtin, 2002, 2000)). For any (mechanical) initial boundary value problem, FDM allows to uniquely determine the elastic and plastic distortion fields by prescribing the areal dislocation density and volume/boundary conditions involving the plastic distortion field (Acharya et al., 2019). In addition, the thermodynamic considerations in FDM straightforwardly result in dislocation driving forces that are crystallographic in nature. Therefore, FDM is the most appropriate approach for the desired strong coupling with heat conduction.

This paper is structured as follows. The notations and tensorial operations used in this work are presented in section 2. In section 3, the proposed model, henceforth known as the thermal-FDM (T-FDM) model, is developed. The model development involves a thorough consideration of the kinematics and thermomechanics of the coupled FDM, thermal quasi-dislocations and heat conduction problem. In the discussion section 4, some consequences of the thermodynamic considerations of the T-FDM model are presented. In addition, some illustrative problems are analytically solved to demonstrate the applicability of the model and better understand the concept of thermal quasi-dislocations and their relationship with dislocations. Concluding remarks are presented in section 5 and the bibliography in section 6.

2. Notations and tensorial operations

Scalars (zeroth order tensors) are denoted with regular font. A first order tensor, i.e. vector, is denoted with a bold and italic lowercase letter. Unit vectors will be denoted with an additional overhead hat symbol ^. Second order tensors are denoted with bold and italic uppercase letters or bold and italic lowercase Greek symbols. Third order tensors are denoted with bold non-italic uppercase letters. Fourth order tensors are denoted with uppercase calligraphic font. Null non-scalar tensorial quantities are represented by equating them to the bold font zero symbol, i.e. $\mathbf{0}$. Whenever the Einstein notation is used, tensors are represented using a non-bold font. The Einstein summation convention will be implied for operations between tensorial quantities; in this section, it is used to understand different tensorial operations considered in this work. Consider two vectors, $\boldsymbol{a}$ and $\boldsymbol{b}$, two second order tensors $\boldsymbol{A}$ and $\boldsymbol{\beta}$, and rectangular Cartesian basis unit vectors $\hat{\boldsymbol{e}}$. In this work, we will use the following operations (demonstrated in the rectangular Cartesian frame).

Tensorial (outer) product:

$$(\boldsymbol{a} \otimes \boldsymbol{b})_{ij} = a_i b_j \hat{e}_i \otimes \hat{e}_j$$
$$(\boldsymbol{a} \otimes \boldsymbol{\beta})_{ijk} = a_i \beta_{jk} \hat{e}_i \otimes \hat{e}_j \otimes \hat{e}_k$$
$$(\boldsymbol{A} \otimes \boldsymbol{b})_{ijk} = A_{ij} b_k \hat{e}_i \otimes \hat{e}_j \otimes \hat{e}_k$$
$$(\boldsymbol{A} \otimes \boldsymbol{\beta})_{ijkl} = A_{ij} \beta_{kl} \hat{e}_i \otimes \hat{e}_j \otimes \hat{e}_k \otimes \hat{e}_l$$

Inner (dot) product between tensors:

$$(\boldsymbol{a} \cdot \boldsymbol{b}) = (\boldsymbol{b} \cdot \boldsymbol{a}) = a_i b_i$$
$$(\boldsymbol{A} \cdot \boldsymbol{\beta})_{ij} = A_{ik} \beta_{kj} \hat{e}_i \otimes \hat{e}_j$$
$$(\boldsymbol{a} \cdot \boldsymbol{\beta})_j = a_i \beta_{ij} \hat{e}_j$$
$$(\boldsymbol{A} \cdot \boldsymbol{b})_i = A_{ij} b_j \hat{e}_i$$
$$(\boldsymbol{A} : \boldsymbol{\beta}) = A_{ij} \beta_{ij}$$

where ":" is the symbol for a double dot product.

Cross product between tensors:

$$(\boldsymbol{a} \times \boldsymbol{b})_i = e_{ijk} a_j b_k \hat{e}_i$$
$$(\boldsymbol{A} \times \boldsymbol{b})_{ij} = e_{jkl} A_{ik} b_l \hat{e}_i \otimes \hat{e}_j$$
$$(\boldsymbol{a} \times \boldsymbol{\beta})_{ij} = e_{ikl} a_k \beta_{lj} \hat{e}_i \otimes \hat{e}_j$$

where e_{ijk} is a component of the third order Levi-Civita permutation tensor $\mathbf{X}$.

For tensorial operations involving the vector differential operator $\boldsymbol{\nabla}$, we will follow the convention used by Salencon (Salencon, 2001) and Acharya (Acharya, 2003):

$$(\boldsymbol{\nabla a})_{ij} = (\mathbf{grad}\, \boldsymbol{a})_{ij} = a_{i,j} \hat{e}_i \otimes \hat{e}_j$$
$$(\boldsymbol{a \nabla})_{ji} = (\mathbf{grad}\, \boldsymbol{a})^T{}_{ji} = a_{j,i} \hat{e}_i \otimes \hat{e}_j$$
$$(\boldsymbol{\nabla A})_{ijk} = (\mathbf{grad}\, \boldsymbol{A})_{ijk} = A_{ij,k} \hat{e}_i \otimes \hat{e}_j \otimes \hat{e}_k$$
$$(\boldsymbol{\nabla} \cdot \boldsymbol{a}) = (\mathbf{div}\, \boldsymbol{a}) = a_{i,i}$$
$$(\boldsymbol{\nabla} \cdot \boldsymbol{A})_i = (\mathbf{div}\, \boldsymbol{A}) = A_{ij,j} \hat{e}_i$$
$$(\boldsymbol{\nabla} \times \boldsymbol{a})_i = (\mathbf{curl}\, \boldsymbol{a})_i = e_{ijk} a_{k,j} \hat{e}_i$$
$$(\boldsymbol{\nabla} \times \boldsymbol{A})_{ij} = (\mathbf{curl}\, \boldsymbol{A})_{ij} = e_{jkl} A_{il,k} \hat{e}_i \otimes \hat{e}_j$$
$$(\boldsymbol{A} \times \boldsymbol{\nabla})_{ij} = (\mathbf{curl}\, \boldsymbol{A})^T{}_{ij} = e_{ikl} A_{lj,k} \hat{e}_i \otimes \hat{e}_j$$

where the superscript T implies transposition.

3. The T-FDM model

In essence, the T-FDM model is a generalization of the isothermal and adiabatic FDM model of Acharya (Acharya, 2004, 2003, 2001) to a transient heterogeneous temperature distribution case via a strong coupling with the heat conduction problem. FDM has been constructed within a continuum framework whose main assumptions are based on the principles of Rational Thermodynamics (RT) (Coleman, 1964; Coleman and Gurtin, 1967; Coleman and Noll, 1960; Coleman and Owen, 1975; Gurtin, 1968; Truesdell, 1984, 1968; Truesdell and Noll, 2004). The proposed coupling will also be performed in the RT framework.

When dealing with heat conduction, the role of entropy and temperature becomes crucial and these entities need to be treated carefully. Following the proofs by Coleman, Owen and Serrin (Coleman et al., 1981; Coleman and Owen, 1974; Serrin, 1979), we know that for cyclic processes and for approximately cyclic processes described within an RT framework, there exists (i) an entropy that is a state function and (ii) an empirical absolute temperature scale. We will assume that all the intended applications of the T-FDM model fall within the category of cyclic or approximately cyclic processes, and hence the aforementioned entropy and temperature always exist. This assumption will allow us to develop the thermodynamic aspects of the T-FDM model, and its implications will be discussed in section 4.

3.1 Deformation fields in presence of continuously represented stationary dislocations within a steady-state temperature field

Let us consider a simply connected body $\mathcal{B}$ with surface $\partial\mathcal{B}$ and assume that it is a single crystal that does not contain any voids or cracks. Let $\mathcal{B}$ be a thermodynamically closed system, i.e. it is allowed to exchange heat and work with its surroundings but not matter. We will suppose that at any instance in time, $\mathcal{B}$ has a heterogeneous temperature distribution due to some combination of steady-state heat-flux and/or temperature boundary conditions as well as some *a priori* unknown and arbitrarily located steady-state heat sources within $\mathcal{B}$. We shall further assume that the local temperature $\theta(\boldsymbol{x})$ is always below solidus at any given instant in time anywhere in $\mathcal{B}$. We will use θ_0 to denote the reference temperature.

It is clear that $\mathcal{B}$ is not in a global thermal equilibrium. However, we shall adopt the local thermodynamic equilibrium hypothesis, which is the first basic tenet of any RT based model. According to

this hypothesis, we assume that every material point in $\mathcal{B}$ is in thermodynamic (thermal, mechanical and chemical) equilibrium, even though globally $\mathcal{B}$ may not be in thermodynamic equilibrium. Based on these considerations, a material point in $\mathcal{B}$ is assumed to represent an ensemble of atoms having a nearly uniform atomic arrangement (allowing for lattice curvatures induced in the presence of dislocations) at a resolution that is coarse enough such that we are just unable to distinguish the underlying atomic order but fine enough that we can distinguish the distortion fields generated by individual dislocations. For each material point, θ is assumed to be uniform across the underlying ensemble of atoms, which is in coherence with the local thermodynamic equilibrium hypothesis.

Let $\mathcal{B}$ contain an arbitrary distribution of continuously represented dislocations. We aim to determine the deformation fields of dislocations within $\mathcal{B}$ far from the boundary $\partial\mathcal{B}$ at an arbitrary instant in time. We assume small displacements and small strains but large temperature differences are allowed. We will assume that the total displacement field $\boldsymbol{u}$ is continuously differentiable everywhere in $\mathcal{B}$ at any instant in time. Note that the presence of a heterogeneous temperature distribution does not preclude such a definition. The total distortion field $\boldsymbol{U}$, defined as the gradient of total displacement:

$$\boldsymbol{U} = \boldsymbol{\nabla u}, \tag{3.1}$$

is a curl-free field that satisfies

$$\boldsymbol{\nabla} \times \boldsymbol{U} = \boldsymbol{0} \tag{3.2}$$

everywhere in $\mathcal{B}$. Equation (3.2) is a necessary condition for integrability of $\boldsymbol{u}$ and a compatibility condition for $\boldsymbol{U}$. The total strain $\boldsymbol{\varepsilon}$, defined as the symmetric component of $\boldsymbol{U}$:

$$\boldsymbol{\varepsilon} = sym\left(\overline{\overline{\boldsymbol{U}}}\right) = \frac{1}{2}(\boldsymbol{\nabla u} + \boldsymbol{u\nabla}), \tag{3.3}$$

satisfies:

$$\boldsymbol{\nabla} \times \boldsymbol{\varepsilon} \times \boldsymbol{\nabla} = \boldsymbol{0} \tag{3.4}$$

everywhere in $\mathcal{B}$, at any instant in time.

In the presence of dislocations in a heterogeneous temperature field, $\boldsymbol{U}$ can be additively decomposed into elastic $\boldsymbol{U}^e$ and inelastic $\boldsymbol{U}^{in}$ components:

$$\boldsymbol{U} = \boldsymbol{U}^e + \boldsymbol{U}^{in}, \tag{3.5}$$

Similarly, $\boldsymbol{\varepsilon}$ can be additively decomposed into elastic $\boldsymbol{\varepsilon}^e$ and inelastic $\boldsymbol{\varepsilon}^{in}$ components as:

$$\boldsymbol{\varepsilon} = \boldsymbol{\varepsilon}^e + \boldsymbol{\varepsilon}^{in}, \tag{3.6}$$

with $\boldsymbol{\varepsilon}^e = sym(\boldsymbol{U}^e)$, $\boldsymbol{\varepsilon}^{in} = sym\left(\boldsymbol{U}^{in}\right)$.

$\boldsymbol{U}^{in}$ has contributions coming from plastic distortion $\boldsymbol{U}^p$ induced by the presence of dislocations and thermal distortion due to the presence of a temperature field $\theta(\boldsymbol{x})$. It is well established that thermal distortion is a symmetric tensor and hence, a pure strain $\boldsymbol{\varepsilon}^\theta$. Kröner (Kröner, 1958) noted that $\boldsymbol{\varepsilon}^\theta(\theta)$ does not result in any repulsive forces, and called it a quasi-plastic distortion field.

$\boldsymbol{U}^{in}$ and $\boldsymbol{U}^{in}$ can be additively decomposed into:

$$\boldsymbol{U}^{in} = \boldsymbol{\varepsilon}^\theta + \boldsymbol{U}^p, \tag{3.7}$$

$$\boldsymbol{\varepsilon}^{in} = \boldsymbol{\varepsilon}^\theta + \boldsymbol{\varepsilon}^p, \tag{3.8}$$

where $\boldsymbol{\varepsilon}^p$ is the plastic strain tensor.

The presence of dislocations induces an incompatibility in $\boldsymbol{U}^p$. The presence of a heterogeneous temperature field under thermal loading and arbitrary local heat sources can induce an incompatibility in $\boldsymbol{\varepsilon}^\theta$. Together, dislocations and a heterogeneous temperature field induce an incompatibility in the elastic distortion $\boldsymbol{U}^e$.

Following (Acharya and Roy, 2006), we invoke the Stokes-Helmholtz decomposition to uniquely decompose $\boldsymbol{U}^e$ and $\boldsymbol{U}^p$ into their respective compatible (curl-free and denoted via the superscript "∥") and incompatible (divergence-free and denoted via the superscript "⊥") components:

$$\boldsymbol{U}^i = \boldsymbol{U}^{i\parallel} + \boldsymbol{U}^{i\perp} = \boldsymbol{\nabla w}^i + \boldsymbol{\chi}^i; i = e, p \tag{3.9}$$

where, in the context of a unique decomposition of a second order tensor $\boldsymbol{U}^i$, one can define unique $\boldsymbol{\nabla w}^i$ and $\boldsymbol{\chi}^i$, subject to appropriate boundary conditions that are defined later (equations (3.16) and (3.20)), whose sum gives back $\boldsymbol{U}^i$; this proves that any second order tensor can be decomposed via the Stokes-Helmholtz decomposition. In practice, one can decompose $\boldsymbol{U}^i$ into such a sum and then determine $\boldsymbol{\nabla w}^i$ and $\boldsymbol{\chi}^i$. Note that $\boldsymbol{U}$ is a compatible field $\boldsymbol{U}^\parallel$ due to its definition in equation (3.2).

The symmetric thermal strain tensor $\boldsymbol{\varepsilon}^\theta$ can also be decomposed uniquely via the Stokes-Helmholtz decomposition as:

$$\boldsymbol{\varepsilon}^\theta = \boldsymbol{U}^{\theta\parallel} + \boldsymbol{U}^{\theta\perp} = \boldsymbol{\nabla w}^\theta + \boldsymbol{\chi}^\theta \tag{3.10a}$$

where $\boldsymbol{U}^{\theta\parallel} = \boldsymbol{\nabla w}^\theta$ and $\boldsymbol{U}^{\theta\perp} = \boldsymbol{\chi}^\theta$ are compatible and incompatible asymmetric tensors, respectively, with the necessary condition that their sum is symmetric, i.e. $\boldsymbol{U}^{\theta\parallel} + \boldsymbol{U}^{\theta\perp} = \left(\boldsymbol{U}^{\theta\parallel} + \boldsymbol{U}^{\theta\perp}\right)^T$. During application of the T-FDM model, we will use the well-established empirical form of $\boldsymbol{\varepsilon}^\theta$:

$$\boldsymbol{\varepsilon}^\theta = \boldsymbol{\gamma}\Delta\theta \tag{3.10b}$$

where $\boldsymbol{\gamma}$ is the local thermal expansion coefficient tensor of order 2, which is symmetric, and $\Delta\theta = \theta - \theta_0$. The importance of performing the Stokes-Helmholtz decomposition of $\boldsymbol{\varepsilon}^\theta$ will become evident later (equation (3.16)).

Note that Kröner (Kröner, 1958) assumed $\boldsymbol{\varepsilon}^\theta$ to be a spherically symmetric tensor $\gamma\Delta\theta\mathbb{I}$; where $\mathbb{I} = \delta_{ij}$ and $\gamma > 0$. This assumption restricts the usage of equation (3.10b) to materials with cubic symmetry. In this work, we allow $\boldsymbol{\gamma}$ to be any positive definite symmetric tensor of order 2. Furthermore, Kröner (Kröner, 1958) also assumed $\gamma\Delta\theta$ to be equal to $\partial^2\Phi/\partial x_i^2$ and $\boldsymbol{\varepsilon}^\theta$ was expressed as $\boldsymbol{\varepsilon}^\theta = \boldsymbol{\nabla\nabla}\Phi + \boldsymbol{\nabla} \times (\Phi\mathbb{I}) \times \boldsymbol{\nabla}$; where Φ is a scalar.

Equations (3.6), (3.8), (3.10a) and (3.10b) imply that

$$\boldsymbol{U}^{e\perp} + \boldsymbol{U}^{in\perp} = \boldsymbol{0}, \tag{3.11}$$

with $\boldsymbol{U}^{in\perp} = \boldsymbol{U}^{p\perp} + \boldsymbol{U}^{\theta\perp}$.

Consider an arbitrary material surface S inside $\mathcal{B}$ and let an ensemble of dislocations and thermal quasi-dislocations thread this surface. In the most general case, the presence of both dislocations and thermal quasi-dislocations precludes a unique definition of the elastic displacement field. If we were to draw a circuit C along the edges of the surface S surrounding dislocations and thermal quasi-dislocations, then a constant discontinuity $\boldsymbol{b}$, in the form of a jump in the elastic displacement $[\![\boldsymbol{u}^e]\!]$, manifests itself as a closure defect along the circuit C such that:

$$\boldsymbol{b} = [\![\boldsymbol{u}^e]\!] = \int_C \boldsymbol{U}^e \cdot \boldsymbol{dl} = \int_C \boldsymbol{U}^{e\perp} \cdot \boldsymbol{dl} = -\int_C \left(\boldsymbol{U}^{p\perp} + \boldsymbol{U}^{\theta\perp}\right) \cdot \boldsymbol{dl} = \boldsymbol{b}^p + \boldsymbol{b}^\theta \tag{3.12}$$

where $\boldsymbol{dl}$ is the local tangent to C, which is a circuit akin to the Burgers circuit. $\boldsymbol{b}^p = -\int_C \boldsymbol{U}^{p\perp} \cdot \boldsymbol{dl}$ is the jump in the elastic displacement induced in the presence of only dislocations, i.e. it is the Burgers vector.

$\boldsymbol{b}^{\theta} = -\int_C \boldsymbol{U}^{\theta\perp} \cdot \boldsymbol{dl}$ is the jump in the elastic displacement induced in the presence of only thermal quasi-dislocations. Thus, $\boldsymbol{b}$ is a vector akin to the Burgers vector that represents the jump in the elastic displacement induced in the presence of dislocations and thermal quasi-dislocations.

Next, using the Stokes' theorem in equation (3.12) we get

$$\boldsymbol{b} = \int_S \boldsymbol{\nabla} \times \boldsymbol{U}^{e} \cdot \hat{\boldsymbol{n}}\, dS = \int_S \boldsymbol{\nabla} \times \boldsymbol{U}^{e\perp} \cdot \hat{\boldsymbol{n}}\, dS = -\int_S \boldsymbol{\nabla} \times \boldsymbol{U}^{p\perp} \cdot \hat{\boldsymbol{n}}\, dS - \int_S \boldsymbol{\nabla} \times \boldsymbol{U}^{\theta\perp} \cdot \hat{\boldsymbol{n}}\, dS, \tag{3.13}$$

where $\hat{\boldsymbol{n}}$ is a unit normal to the surface S. Defining pointwise continuous second order tensor fields $\boldsymbol{\alpha}$, $\boldsymbol{\alpha}^{p}$ and $\boldsymbol{\alpha}^{\theta}$ as

$$\boldsymbol{\alpha} = \boldsymbol{\nabla} \times \boldsymbol{U}^{e} = \boldsymbol{\nabla} \times \boldsymbol{U}^{e\perp} = -\boldsymbol{\nabla} \times \boldsymbol{U}^{in} = -\boldsymbol{\nabla} \times \boldsymbol{U}^{p} - \boldsymbol{\nabla} \times \boldsymbol{\varepsilon}^{\theta} = -\boldsymbol{\nabla} \times \boldsymbol{U}^{p\perp} - \boldsymbol{\nabla} \times \boldsymbol{U}^{\theta\perp} = \boldsymbol{\alpha}^{p} + \boldsymbol{\alpha}^{\theta}, \tag{3.14}$$

$$\boldsymbol{\alpha}^{p} = -\boldsymbol{\nabla} \times \boldsymbol{U}^{p} = -\boldsymbol{\nabla} \times \boldsymbol{U}^{p\perp}, \tag{3.15}$$

$$\boldsymbol{\alpha}^{\theta} = -\boldsymbol{\nabla} \times \boldsymbol{\varepsilon}^{\theta} = -\boldsymbol{\nabla} \times \boldsymbol{U}^{\theta\perp}, \tag{3.16}$$

respectively, we get

$$\boldsymbol{b} = \int_S \boldsymbol{\alpha} \cdot \hat{\boldsymbol{n}}\, dS = \int_S \boldsymbol{\alpha}^{p} \cdot \hat{\boldsymbol{n}}\, dS + \int_S \boldsymbol{\alpha}^{\theta} \cdot \hat{\boldsymbol{n}}\, dS = \boldsymbol{b}^{p} + \boldsymbol{b}^{\theta} \tag{3.17}$$

$\boldsymbol{\alpha}$ is better known as the Nye's tensor (Nye, 1953). Equation (3.14) reveals two distinct contributions to the Nye's tensor. The first contribution comes from the presence of dislocations whose areal density is represented by the dislocation density tensor $\boldsymbol{\alpha}^{p}$. While $\boldsymbol{\alpha}^{p}$ does not dependent on $\boldsymbol{U}^{\theta\perp}$, it is nevertheless affected by the local θ through its effect on the magnitudes of the Burgers and line vectors. The second contribution comes from thermal quasi-dislocations whose areal density is represented by $\boldsymbol{\alpha}^{\theta}$, which arises purely from $\boldsymbol{U}^{\theta\perp}$. It is clear that $\boldsymbol{b}^{p} = \int_S \boldsymbol{\alpha}^{p} \cdot \hat{\boldsymbol{n}}\, dS$ and $\boldsymbol{b}^{\theta} = \int_S \boldsymbol{\alpha}^{\theta} \cdot \hat{\boldsymbol{n}}\, dS$. Note that in conventional dislocation mechanics, where the thermal quasi-dislocation density is not considered, $\boldsymbol{\alpha} = \boldsymbol{\alpha}^{p}$. In the sole presence of thermal quasi-dislocations, $\boldsymbol{\alpha} = \boldsymbol{\alpha}^{\theta}$. Equation (3.14) also allows the possibility that $\boldsymbol{\alpha}^{p} = -\boldsymbol{\alpha}^{\theta}$ when $\boldsymbol{\alpha} = \boldsymbol{0}$.

From equations (3.14) – (3.16), we obtain the following continuity conditions,

$$\boldsymbol{\nabla} \cdot \boldsymbol{\alpha} = 0, \boldsymbol{\nabla} \cdot \boldsymbol{\alpha}^{p} = 0 \text{ and } \boldsymbol{\nabla} \cdot \boldsymbol{\alpha}^{\theta} = 0 \tag{3.18}$$

When it comes to determining $\boldsymbol{U}^{e\perp}$ from $\boldsymbol{\alpha}$, equation (3.14) is insufficient because it does not ensure that $\boldsymbol{U}^{e\perp}$ is equal to zero in the absence of $\boldsymbol{\alpha}$, which should be the case. Following (Acharya et al., 2019; Acharya and Roy, 2006), equation (3.14) needs to be augmented with additional conditions,

$$\boldsymbol{\nabla} \cdot \boldsymbol{U}^{e\perp} = \boldsymbol{0} \text{ in } \mathcal{B} \tag{3.19a}$$

$$\boldsymbol{U}^{e\perp} \cdot \hat{\boldsymbol{n}} = \boldsymbol{0} \text{ on } \partial\mathcal{B} \tag{3.19b}$$

In equation set (3.19), the latter condition is imposed to ensure that its solution does not contain a gradient term. Taking the curl of equation (3.14) and using equation set (3.19) we get,

$$\boldsymbol{\nabla} \cdot \boldsymbol{\nabla}\boldsymbol{U}^{e\perp} = -\boldsymbol{\nabla} \times \boldsymbol{\alpha} \text{ in } \mathcal{B} \tag{3.20a}$$

$$\boldsymbol{U}^{e\perp} \cdot \hat{\boldsymbol{n}} = \boldsymbol{0} \text{ on } \partial\mathcal{B} \tag{3.20b}$$

The left-hand side of equation (3.20a) is a Poisson type equation whose solution for $\boldsymbol{U}^{e\perp}$ under the given boundary condition vanishes when $\boldsymbol{\alpha} = \boldsymbol{0}$.

We can follow a similar procedure to deduce the following conditions for $\boldsymbol{U}^{p\perp}$ and $\boldsymbol{U}^{\theta\perp}$:

$$\boldsymbol{\nabla} \cdot \boldsymbol{\nabla}\boldsymbol{U}^{p\perp} + \boldsymbol{\nabla} \cdot \boldsymbol{\nabla}\boldsymbol{U}^{\theta\perp} = \boldsymbol{\nabla} \times \boldsymbol{\alpha} \text{ in } \mathcal{B}, \tag{3.21a}$$

$$\boldsymbol{U}^{p\perp} \cdot \hat{\boldsymbol{n}} = \boldsymbol{0} \quad \text{and} \quad \boldsymbol{U}^{\theta\perp} \cdot \hat{\boldsymbol{n}} = \boldsymbol{0} \text{ on } \partial\mathcal{B}, \tag{3.21b}$$

which are obtained from $\boldsymbol{\nabla} \cdot \boldsymbol{U}^{p\perp} = \boldsymbol{0}$ and $\boldsymbol{\nabla} \cdot \boldsymbol{U}^{\theta\perp} = \boldsymbol{0}$.

When it comes to determining $\boldsymbol{b}^{\theta}$ from known $\boldsymbol{\alpha}^{\theta}$ or $\boldsymbol{U}^{\theta\perp}$ in the presence of strong thermal gradients, special attention must be given to the shape and size of surface S and circuit C, which will determine whether $\boldsymbol{b}^{\theta}$ depend only on the local temperature θ or on the temperature distribution in the neighborhood within S (delimited by C). In this work, we shall concern ourselves with the case where $\boldsymbol{b}^{\theta}$ depends only on the local θ. This implies that in the presence of strong thermal gradients, the shape and size of S cannot be larger than the largest possible surface in the underlying ensemble of atoms at a material point in $\mathcal{B}$. As a consequence, $\boldsymbol{b}$ will also depend on the local θ. Now, the same S and C will be used to determine $\boldsymbol{b}^{\theta}$, $\boldsymbol{b}^{p}$ and $\boldsymbol{b}$. This implies that for most cases considered during the application of the T-FDM model only one dislocation may traverse S at a given point in time. Occasionally, a few dislocations, each on a different slip system, may traverse S. Rarely, more than one dislocation on a slip system would traverse S.

We are also interested in connecting the above developments with the crystallography of the material. This requires associating dislocations with a slip system based on their slip plane and direction. Let $\boldsymbol{\alpha}^{p,\beta}$ represent the density of a dislocation that can glide on a slip system β. If this dislocation crosses a surface S, then from equation (3.15) we get the Burgers vector of this dislocation as $\boldsymbol{b}^{p,\beta} = \int_S \boldsymbol{\alpha}^{p,\beta} \cdot \hat{\boldsymbol{n}}\, dS$. If $\boldsymbol{l}^{p,\beta}$ is the local tangent to this dislocation line, then $\boldsymbol{\alpha}^{p,\beta}$ can be written as:

$$\boldsymbol{\alpha}^{p,\beta} = \frac{1}{V}\left(\boldsymbol{b}^{p,\beta} \otimes \boldsymbol{l}^{p,\beta}\right) \tag{3.22}$$

where V is a reference volume that should be chosen such that variations in θ within this volume are negligible; based on the discussion after equation set (3.21), V corresponds to the volume of the underlying ensemble of atoms at a material point in $\mathcal{B}$. This dislocation together with thermal quasi-dislocations within the volume V would contribute to the Nye's tensor and Burgers vector as follows:

$$\boldsymbol{\alpha} = \boldsymbol{\alpha}^{p,\beta} + \boldsymbol{\alpha}^{\theta} = \frac{1}{V}\left(\boldsymbol{b}^{p,\beta} \otimes \boldsymbol{l}^{p,\beta}\right) + \boldsymbol{\alpha}^{\theta} \tag{3.23a}$$

$$\boldsymbol{b} = \boldsymbol{b}^{p,\beta} + \boldsymbol{b}^{\theta} \tag{3.23b}$$

where $\boldsymbol{b}^{\theta} = \int_S \boldsymbol{\alpha}^{\theta} \cdot \hat{\boldsymbol{n}}\, dS$. Note that the manner in which the model is constructed allows us to characterize thermal quasi-dislocations via an "equivalent to a Burgers vector". However, attributing a line direction to this defect is not allowed because thermal quasi-dislocations do not manifest as line crystal defects.

If there are multiple dislocations on the same slip system β that traverse S, then $\boldsymbol{b}^{p,\beta}$ and $\boldsymbol{\alpha}^{p,\beta}$ in equation set (3.23) determine the net Burgers vector and density tensor, respectively, of the ensemble of these dislocations.

If multiple dislocations from different slip systems traverse S, then their net local Burgers vector $\boldsymbol{b}^{p} = \sum_{\beta} \boldsymbol{b}^{p,\beta} = \sum_{\beta} \int_S \boldsymbol{\alpha}^{p,\beta} \cdot \hat{\boldsymbol{n}}\, dS = \int_S \left(\sum_{\beta} \boldsymbol{\alpha}^{p,\beta}\right) \cdot \hat{\boldsymbol{n}}\, dS = \int_S \boldsymbol{\alpha}^{p} \cdot \hat{\boldsymbol{n}}\, dS$; the sum is over all slip systems β at a given material point. For this configuration, the Nye's tensor $\boldsymbol{\alpha}$ and Burgers vector $\boldsymbol{b}$ are:

$$\boldsymbol{\alpha} = \boldsymbol{\alpha}^{p} + \boldsymbol{\alpha}^{\theta} = \frac{1}{V}\sum_{\beta}\left(\boldsymbol{b}^{p,\beta} \otimes \boldsymbol{l}^{p,\beta}\right) + \boldsymbol{\alpha}^{\theta} \tag{3.24a}$$

$$\boldsymbol{b} = \sum_{\beta} \boldsymbol{b}^{p,\beta} + \boldsymbol{b}^{\theta} \tag{3.24b}$$

Finally, we note that under steady-state heat conduction, the temperature field $\theta(\boldsymbol{x})$ does not evolve in time. Consequently, in the absence of mechanical loading, immobile dislocations will continue to remain immobile and no new dislocations will be generated. In this case, the condition $\frac{\partial}{\partial t}\int_S \boldsymbol{\alpha} \cdot \hat{\boldsymbol{n}}\, dS = 0$ needs to be satisfied for all surfaces S in $\mathcal{B}$.

3.2 Kinematics of continuously represented stationary dislocations in a transient heterogeneous temperature field

Let us now assume that the heat flux and/or temperature boundary conditions evolve with time but the dislocations in $\mathcal{B}$ remain immobile. An evolving temperature field naturally entails an evolving $\boldsymbol{\varepsilon}^{\theta}$. Consequently, the thermal quasi-dislocations will also evolve with time via $\dot{\boldsymbol{\alpha}}^{\theta} = -\boldsymbol{\nabla} \times \dot{\boldsymbol{\varepsilon}}^{\theta} = -\boldsymbol{\nabla} \times \dot{\boldsymbol{U}}^{\theta\perp}$. Since we have assumed $\boldsymbol{\varepsilon}^{\theta}$ has the relationship (3.9), we obtain $\dot{\boldsymbol{\alpha}}^{\theta} = \frac{\partial}{\partial t}[\boldsymbol{\nabla} \times (\boldsymbol{\gamma}\Delta\theta)] = (\boldsymbol{\nabla} \times \dot{\boldsymbol{\gamma}})\Delta\theta + (\boldsymbol{\nabla} \times \boldsymbol{\gamma})\dot{\theta} - \dot{\boldsymbol{\gamma}} \cdot [\boldsymbol{\nabla}\theta \cdot \mathbf{X}] - \boldsymbol{\gamma} \cdot \left[\frac{\partial}{\partial t}(\boldsymbol{\nabla}\theta) \cdot \mathbf{X}\right]$. If we assume that $\boldsymbol{\gamma}$ does not evolve in space and time, then $\dot{\boldsymbol{\alpha}}^{\theta} = -\boldsymbol{\gamma} \cdot \left[\frac{\partial}{\partial t}(\boldsymbol{\nabla}\theta) \cdot \mathbf{X}\right]$.

The local dislocation density $\boldsymbol{\alpha}^{p,\beta}$ evolves in its magnitude and spread because of the dependence of the Burgers and line vectors on the evolving local temperature (equation (3.22)). A change in the magnitude of the dislocation density can be thought of as the local generation/annihilation of dislocations without their motion. This can be represented via a local dislocation source/sink term that also evolves the density of existing dislocations, say $\boldsymbol{S}^{p,\beta}$, such that $\dot{\boldsymbol{\alpha}}^{p,\beta} = \boldsymbol{S}^{p,\beta}$; if no dislocations exist in the body and no dislocations are generated, then $\dot{\boldsymbol{\alpha}}^{p,\beta} = \boldsymbol{S}^{p,\beta} = \mathbf{0}$ for all slip systems everywhere in the body. For multiple dislocations on different slip systems, we can combine their source terms to have $\boldsymbol{S}^{p} = \sum_{\beta} \boldsymbol{S}^{p,\beta}$ and $\dot{\boldsymbol{\alpha}}^{p} = \boldsymbol{S}^{p}$. In the case of existing dislocations, we will assume that only the magnitude of their Burgers and line vectors would evolve with time and let $\boldsymbol{S}^{p,\beta} = \left[\widehat{\boldsymbol{b}}^{p,\beta} \otimes \widehat{\boldsymbol{l}}^{p,\beta}\right]\frac{\partial}{\partial t}\left(\frac{|\boldsymbol{b}^{p,\beta}||\boldsymbol{l}^{p,\beta}|}{V}\right)$, where $\widehat{\boldsymbol{b}}^{p,\beta}$ and $\widehat{\boldsymbol{l}}^{p,\beta}$ are unit Burgers and line vectors, respectively. Note that an evolving dislocation density entails an evolving $\boldsymbol{U}^{p\perp}$, however, it does not imply an evolution of $\boldsymbol{U}^{p\parallel}$ because $\boldsymbol{U}^{p\parallel}$ is associated with the history of dislocation motion (Acharya, 2001), which in this case remains unchanged.

Incompatible elastic distortions $\boldsymbol{U}^{e\perp}$ may or may not evolve with time. In the former case, the stress field associated with the dislocations and thermal quasi-dislocations may also evolve in time; a constitutive relationship for the stress field is given later in section 3.8. In the latter case, there will not be any change in the stress field. Furthermore, from equation (3.14), we can derive $\boldsymbol{S}^{p} = -\dot{\boldsymbol{\alpha}}^{\theta}$, which implies that dislocations are being generated, annihilated or their densities are evolving due to temperature changes, however, there will be no dislocation motion.

Based on the above considerations and equations (3.10), (3.11), (3.14) and (3.19) we can deduce the following relationships for the case of transient heat conduction in a body containing stationary dislocations:

$$\left.\begin{array}{c} \dot{\boldsymbol{\alpha}}^{p} = -\boldsymbol{\nabla} \times \dot{\boldsymbol{U}}^{p} = -\boldsymbol{\nabla} \times \dot{\boldsymbol{U}}^{p\perp} = \boldsymbol{S}^{p} = \sum_{\beta} \dot{\boldsymbol{\alpha}}^{p,\beta} = \sum_{\beta} \boldsymbol{S}^{p,\beta} \\ \dot{\boldsymbol{\alpha}}^{\theta} = -\boldsymbol{\nabla} \times \dot{\boldsymbol{\varepsilon}}^{\theta} = -\boldsymbol{\nabla} \times \dot{\boldsymbol{U}}^{\theta\perp} = (\boldsymbol{\nabla} \times \dot{\boldsymbol{\gamma}})\Delta\theta + (\boldsymbol{\nabla} \times \boldsymbol{\gamma})\dot{\theta} - \dot{\boldsymbol{\gamma}} \cdot [\boldsymbol{\nabla}(\Delta\theta) \cdot \mathbf{X}] - \boldsymbol{\gamma} \cdot \left[\boldsymbol{\nabla}(\dot{\Delta}\theta) \cdot \mathbf{X}\right] \\ \dot{\boldsymbol{\alpha}} = \boldsymbol{\nabla} \times \dot{\boldsymbol{U}}^{e\perp} = \dot{\boldsymbol{\alpha}}^{p} + \dot{\boldsymbol{\alpha}}^{\theta} = \sum_{\beta} \boldsymbol{S}^{p,\beta} - \dot{\boldsymbol{\alpha}}^{\theta} \\ \dot{\boldsymbol{U}}^{p\parallel} = \mathbf{0} \end{array}\right\} \quad (3.25)$$

3.3 Kinematics of continuously represented mobile dislocations in a transient heterogeneous temperature field

Let us now assume that $\mathcal{B}$ is subjected to a thermo-elastic-plastic deformation under the action of some transient traction and/or displacement as well as heat flux and/or temperature boundary conditions. We are now considering the case of mobile dislocations.

We adopt the approach of (Acharya, 2011) to derive the dynamic equation of dislocation motion. We follow the temporal evolution of the Burgers vector content within a circuit $C(t)$ bounding an arbitrary curved area patch $S(t)$ in $\mathcal{B}$, which is sufficiently small to have a uniform θ within the region bounded by

this surface; note that C and S may evolve in time. We will assume that $S(t)$ is traversed by a dislocation on a slip system β at a velocity $\boldsymbol{v}^{\beta}$ with respect to the material. We will also account for $\boldsymbol{S}^{p,\beta}(\theta)$ (seen in section 3.2) arising from local temperature changes. The associated equation for the dynamics of dislocations is:

$$\frac{\partial}{\partial t}\int_{S(t)} \boldsymbol{\alpha}^{p,\beta} \cdot \hat{\boldsymbol{n}}\, dS = -\int_{C(t)} \left(\boldsymbol{\alpha}^{p,\beta} \times \boldsymbol{v}^{\beta}\right) \cdot \boldsymbol{dx} + \int_{S(t)} \boldsymbol{S}^{p,\beta} \cdot \hat{\boldsymbol{n}}\, dS$$
$$= -\int_{S(t)} \left[\boldsymbol{\nabla} \times \left(\boldsymbol{\alpha}^{p,\beta} \times \boldsymbol{v}^{\beta}\right) + \boldsymbol{S}^{p,\beta}\right] \cdot \hat{\boldsymbol{n}} \tag{3.26}$$

Equation (3.26) is similar to the expression proposed in (Acharya, 2011, 2003); a detailed explanation for the origin of the right hand side of this equation can be found in these references.

In the local form, equation (3.26) reads:

$$\dot{\boldsymbol{\alpha}}^{p,\beta} = -\boldsymbol{\nabla} \times \left(\boldsymbol{\alpha}^{p,\beta} \times \boldsymbol{v}^{p,\beta}\right) + \boldsymbol{S}^{p,\beta} \tag{3.27}$$

Let $\overline{\overline{\widetilde{\boldsymbol{U}}}}^{p,\beta}(\theta)$ be the local slip distortion tensor associated with the motion of a mobile dislocation on slip system β. The rate of change of $\widetilde{\boldsymbol{U}}^{p,\beta}$ with respect to time can be written as:

$$\dot{\widetilde{\boldsymbol{U}}}^{p,\beta} = \boldsymbol{\alpha}^{p,\beta} \times \boldsymbol{v}^{\beta}, \tag{3.28}$$

which is unique up to a gradient term. The rate of change of the Nye's tensor can then be obtained from equation (3.27) as:

$$\dot{\boldsymbol{\alpha}} = \dot{\boldsymbol{\alpha}}^{p,\beta} + \dot{\boldsymbol{\alpha}}^{\theta} = -\boldsymbol{\nabla} \times \left(\boldsymbol{\alpha}^{p,\beta} \times \boldsymbol{v}^{\beta}\right) + \boldsymbol{S}^{p,\beta} + \dot{\boldsymbol{\alpha}}^{\theta} \tag{3.29}$$

Equation (3.29) reveals an intimate relationship between dislocation motion, dislocation density generation/annihilation/evolution without motion due to temperature changes, and thermal quasi-dislocation density evolution. It can be best appreciated when $\dot{\boldsymbol{\alpha}} = \boldsymbol{0}$. In this case, on one hand, we have $\dot{\boldsymbol{\alpha}}^{p,\beta} = -\dot{\boldsymbol{\alpha}}^{\theta}$. This equation implies that the incompatibility in elastic distortion does not evolve during temperature changes if the change in thermal quasi-dislocation density associated with the temperature change is accommodated through the generation, annihilation and/or motion of dislocations. On the other hand, we can view the same equation as $\dot{\boldsymbol{\alpha}}^{\theta} = \boldsymbol{\nabla} \times \left(\boldsymbol{\alpha}^{p,\beta} \times \boldsymbol{v}^{\beta}\right) - \boldsymbol{S}^{p,\beta}$. This relationship implies that dislocation motion can result in the evolution of thermal quasi-dislocation density and incompatible thermal strains, which would affect the local temperature. However, the appropriate equation for temperature evolution must come from thermodynamic considerations, which is demonstrated later via equation (3.57) in section 3.10.

Equation (3.29) also indicates that since $\dot{\boldsymbol{\alpha}}^{\theta}$ is not associated with any particular slip system, its evolution may also result in the evolution of dislocations on different slip systems. Therefore, this equation has to be generalized to the case of multiple dislocations on different slip systems. If multiple dislocations on different slip systems are passing through a material point, then the net slip distortion tensor rate due to all these dislocations is given as:

$$\dot{\widetilde{\boldsymbol{U}}}^{p} = \sum_{\beta} \dot{\widetilde{\boldsymbol{U}}}^{p,\beta} = \sum_{\beta} \left(\boldsymbol{\alpha}^{p,\beta} \times \boldsymbol{v}^{p,\beta}\right) \tag{3.30}$$

For this case, the rate of change of the Nye's tensor is given by:

$$\dot{\boldsymbol{\alpha}} = \sum_{\beta} \left(\dot{\boldsymbol{\alpha}}^{p,\beta}\right) + \dot{\boldsymbol{\alpha}}^{\theta} = -\sum_{\beta} \left[\boldsymbol{\nabla} \times \left(\boldsymbol{\alpha}^{p,\beta} \times \boldsymbol{v}^{p,\beta}\right) - \boldsymbol{S}^{p,\beta}\right] + \dot{\boldsymbol{\alpha}}^{\theta} \tag{3.31}$$

Equation (3.31) is the most general form for the relationship between the evolutions of dislocation and thermal quasi-dislocation densities. In addition to the observations that can be made from equation (3.29), equation (3.31) indicates that dislocation motion on any slip system can result in the evolution of the thermal quasi-dislocation density. Whereas the evolution of thermal quasi-dislocations can result in the

motion of dislocations on other slip systems, including on those that are "inactive" based on restrictions imposed by crystallography and local stress conditions. Furthermore, if $\boldsymbol{v}^{p,\beta}$ has an out-of-slip-plane component, then cross-slip, climb and non-Schmid mechanisms could also occur (Acharya, 2003).

In a more general case, dislocation motion, generation and annihilation along with the evolution of thermal quasi-dislocations would also be accompanied by the evolution of $\boldsymbol{U}^{e\perp}$ via a non-zero $\dot{\boldsymbol{\alpha}}$. It is through this possibility that equations (3.29) and (3.31) could allow the presence of stationary dislocations in a field of evolving thermal quasi-dislocations.

Finally, note that while we have $\boldsymbol{U}^{p,\beta} = \widetilde{\boldsymbol{U}}^{p,\beta}$ for a slip system β, typically $\boldsymbol{U}^{p} \neq \widetilde{\boldsymbol{U}}^{p}$ in the case where multiple dislocations on different slip systems are involved. For the case of traction boundary conditions, we can assume that (Acharya et al., 2019):

$$\boldsymbol{U}^{p\parallel} = \widetilde{\boldsymbol{U}}^{p\parallel} \tag{3.32}$$

3.4 Boundary conditions for thermomechanical loadings

Let $\mathcal{B}$ undergo the aforementioned thermo-elastic-plastic deformation under the action of evolving traction $\boldsymbol{t}$ on surface $\partial\mathcal{B}_t$, displacement $\boldsymbol{u}_d$ on surface $\partial\mathcal{B}_d$, heat flux q_h on surface $\partial\mathcal{B}_q$ and temperature θ' on surface $\partial\mathcal{B}_\theta$.

$$\boldsymbol{t} = \boldsymbol{\sigma}\cdot\hat{\boldsymbol{n}}, \forall \boldsymbol{x} \in \partial\mathcal{B}_t \tag{3.33a}$$

$$\boldsymbol{u} = \boldsymbol{u}_d, \forall \boldsymbol{x} \in \partial\mathcal{B}_d \tag{3.33b}$$

$$q_h = \boldsymbol{q}\cdot\hat{\boldsymbol{n}}, \forall \boldsymbol{x} \in \partial B_q \tag{3.33c}$$

$$\theta = \theta', \forall \boldsymbol{x} \in \partial B_\theta \tag{3.33d}$$

$\boldsymbol{\sigma}$ is the symmetric Cauchy stress tensor. Note that $\partial\mathcal{B}_t \cap \partial\mathcal{B}_d = \emptyset$ and $\partial\mathcal{B}_q \cap \partial\mathcal{B}_\theta = \emptyset$ must be respected. However, $\partial\mathcal{B}_t \cap \partial\mathcal{B}_q$, $\partial\mathcal{B}_t \cap \partial\mathcal{B}_\theta$, $\partial\mathcal{B}_d \cap \partial\mathcal{B}_q$ or $\partial\mathcal{B}_d \cap \partial\mathcal{B}_\theta$ may not be empty sets.

The following condition, which follows from equations (3.18b) and (3.20), has to be satisfied everywhere on $\partial\mathcal{B}$:

$$\boldsymbol{U}^{e\perp}\cdot\hat{\boldsymbol{n}} = \boldsymbol{U}^{p\perp}\cdot\hat{\boldsymbol{n}} = \boldsymbol{U}^{\theta\perp}\cdot\hat{\boldsymbol{n}} = 0 \text{ on } \partial B \tag{3.33e}$$

In addition, one must satisfy the condition $\dot{\widetilde{\boldsymbol{U}}}^{p,\beta}\cdot\hat{\boldsymbol{n}}$ for all slip systems β on ∂B, which yields:

$$\left(\boldsymbol{\nabla}\dot{\boldsymbol{z}}^{p,\beta} - \boldsymbol{\alpha}^{p,\beta}\times\boldsymbol{v}^{p,\beta}\right)\cdot\hat{\boldsymbol{n}} = 0, \forall \boldsymbol{x} \in \partial B \tag{3.33f}$$

where $\boldsymbol{\nabla}\dot{\boldsymbol{z}}^{p,\beta} = \dot{\widetilde{\boldsymbol{U}}}^{p,\beta\parallel}$ and $\dot{\boldsymbol{z}}^{p,\beta}$ need to be prescribed in at least one point in $\mathcal{B}$ (Acharya and Roy, 2006).

In order to obtain a unique solution to equation (3.27) for each slip system, Acharya (Acharya, 2003) proposed the following condition for the flux $\boldsymbol{F}$ of dislocation density on $\partial\mathcal{B}$:

$$\boldsymbol{F}^{\beta} = \boldsymbol{\alpha}^{p,\beta}\left(\boldsymbol{v}^{\beta}\cdot\hat{\boldsymbol{n}}\right), \forall \boldsymbol{x} \in \partial B \tag{3.33g}$$

with $\boldsymbol{v}^{\beta}\cdot\hat{\boldsymbol{n}} \leq 0$ to ensure that there is not outflux of dislocations from $\mathcal{B}$ to the surroundings. This condition can also be applied to equations (3.29) and (3.31) because the term associated with dislocation flux remains the same as in equation (3.27).

Finally, note that since there is no motion of thermal quasi-dislocations, conditions akin to equations (3.33f) and (3.33g) are not required for $\boldsymbol{\alpha}^{\theta}$.

3.5 Balance of linear momentum

Under the sudden application of a large q_h or θ on ∂B_q or ∂B_θ for a short duration of time, a large temperature gradient field can be generated in $\mathcal{B}$ that can result in very rapid changes in local momentum during this short interval in time. We can write the local form of the balance of linear momentum as:

$$\rho\ddot{\boldsymbol{u}} = \boldsymbol{\nabla}\cdot\boldsymbol{\sigma} + \rho\boldsymbol{f}_v \tag{3.34}$$

where ρ (local density), $\boldsymbol{f}_v$ (local force in the volume/body) and $\boldsymbol{\sigma}$ also depend on θ.

3.6 Balance of energy

From the first law of thermodynamics, we obtain the following expression for the local form of the rate of change of internal energy density (u):

$$\rho\dot{u} = -\boldsymbol{\nabla}\cdot\boldsymbol{q} + \boldsymbol{\sigma}:\dot{\boldsymbol{\varepsilon}} + \rho r \tag{3.35}$$

where ρr is representative of internal heat sources, losses to the surroundings, etc.

3.7 Thermo-mechanical dissipation

In order to obtain constitutive relationships for $\boldsymbol{q}$ and $\boldsymbol{\sigma}$ as well as the driving forces for slip-system dislocation velocities $\boldsymbol{v}^{\beta}$, we perform a dissipation analysis based on the second law of thermodynamics. The second basic tenet of any RT based model is to apply the second law in the form of the classical Clausius-Kelvin-Planck inequality (Truesdell and Toupin, 1960), which formulates the entropy change for a system undergoing an irreversible process that brings it from one *equilibrium state* A to another *equilibrium state* B such that:

$$\Delta S \geq \int_A^B \frac{\delta Q}{\theta} \tag{3.36}$$

where ΔS is the entropy change in $\mathcal{B}$, and δQ is the path dependent heat exchanged between $\mathcal{B}$ and its surroundings. Since the total quantity of heat δQ results from the exchange with the surroundings through the boundaries and the presence of internal sources, equation (3.36) can be rewritten as:

$$\frac{\partial}{\partial t}\int_{\mathcal{B}} \rho s \, dV \geq -\int_{\partial\mathcal{B}} \frac{1}{\theta}\boldsymbol{q}\cdot\hat{\boldsymbol{n}}\, dS + \int_{\mathcal{B}} \rho\frac{r}{\theta}\, dV \tag{3.37}$$

where s is the specific entropy and $\rho\frac{r}{\theta}$ corresponds to internal thermal sources of entropy. In local form, this equation can be written as:

$$\rho\dot{s} + \boldsymbol{\nabla}\cdot\frac{\boldsymbol{q}}{\theta} - \rho\frac{r}{\theta} \geq 0 \tag{3.38}$$

Next, eliminating r between equations (3.35) and (3.38) and introducing the Helmholtz free energy density ψ as the Legendre transformation of u with respect to s, i.e. $\psi = u - \theta s$, we obtain the local dissipation inequality:

$$-\rho\left(\dot{\psi} + s\dot{\theta}\right) + \boldsymbol{\sigma}:\dot{\boldsymbol{\varepsilon}} - \frac{1}{\theta}(\boldsymbol{q}\cdot\boldsymbol{\nabla}\theta) \geq 0 \tag{3.39}$$

Inequality (3.39) is known as the Clausius-Duhem inequality.

3.8 Free energy density and energetic constitutive relationships

The free energy density ψ can be taken as a function of the elastic strain and $\boldsymbol{a}$, the set of internal variables, such that $\psi = \hat{\psi}(\boldsymbol{\varepsilon}^e, \boldsymbol{a})$. Following (Coleman and Mizel, 1963), we know that ψ is independent of $\boldsymbol{\nabla}\theta$ and higher gradients of θ, i.e. $\boldsymbol{\nabla}^n\theta, n \geq 2$.

Recalling from equation (3.7) that $\boldsymbol{\varepsilon}^e = \boldsymbol{\varepsilon} - \boldsymbol{\varepsilon}^p - \boldsymbol{\varepsilon}^\theta$, we have $\psi \equiv \hat{\psi}\left(\boldsymbol{\varepsilon} - \boldsymbol{\varepsilon}^p - \boldsymbol{\varepsilon}^\theta, \boldsymbol{a}\right) \equiv \hat{\psi}(\boldsymbol{\varepsilon} - \boldsymbol{\varepsilon}^p, \theta, \boldsymbol{a})$. The time derivative of ψ can be defined as:

$$\dot{\psi} = \frac{\partial\psi}{\partial(\boldsymbol{\varepsilon}-\boldsymbol{\varepsilon}^p)}:(\dot{\boldsymbol{\varepsilon}} - \dot{\boldsymbol{\varepsilon}}^p) + \frac{\partial\psi}{\partial\theta}\dot{\theta} + \frac{\partial\psi}{\partial\boldsymbol{a}}\cdot\dot{\boldsymbol{a}} \tag{3.40}$$

where the dot in $\frac{\partial\psi}{\partial\boldsymbol{a}}\cdot\dot{\boldsymbol{a}}$ represents appropriate number of inner products corresponding to the tensorial order of $\boldsymbol{a}$. Substituting equation (3.40) in (3.39), adding and subtracting $\boldsymbol{\sigma}:\dot{\boldsymbol{\varepsilon}}^p$, and rearranging terms gives:

$$-\left(\rho\frac{\partial\psi}{\partial(\boldsymbol{\varepsilon}-\boldsymbol{\varepsilon}^p)}-\boldsymbol{\sigma}\right):(\dot{\boldsymbol{\varepsilon}}-\dot{\boldsymbol{\varepsilon}}^p)-\rho\left(\frac{\partial\psi}{\partial\theta}+s\right)\dot{\theta}-\rho\frac{\partial\psi}{\partial\boldsymbol{a}}\cdot\dot{\boldsymbol{a}}+\boldsymbol{\sigma}:\dot{\boldsymbol{\varepsilon}}^p-\frac{1}{\theta}(\boldsymbol{q}\cdot\boldsymbol{\nabla}\theta)\geq 0 \tag{3.41}$$

For the inequality (3.41) to hold, the following conditions need to be satisfied (Coleman and Gurtin, 1967):

$$\boldsymbol{\sigma}=\frac{\partial(\rho\psi)}{\partial(\boldsymbol{\varepsilon}-\boldsymbol{\varepsilon}^p)} \tag{3.42}$$

$$s=-\frac{1}{\rho}\frac{\partial(\rho\psi)}{\partial\theta} \tag{3.43}$$

Note that the term $-\rho\frac{\partial\psi}{\partial\boldsymbol{a}}\cdot\dot{\boldsymbol{a}}$ is known as internal dissipation and in the general case:

$$\frac{\partial\psi}{\partial\boldsymbol{a}}\neq 0 \tag{3.44}$$

In this work, we shall restrict ourselves to the case where ψ is independent of $\boldsymbol{a}$, i.e. $\psi=\hat{\psi}(\boldsymbol{\varepsilon}^e)=\hat{\psi}(\boldsymbol{\varepsilon}-\boldsymbol{\varepsilon}^p,\theta)$; note that dependence on internal variables can also be considered (Acharya, 2011), however, it is not necessary for present purposes. Note also that additional terms, similar to the ones proposed in (Acharya and Tartar, 2011; Zhang et al., 2015), need to be accounted for in order to appropriately treat the dislocation core and associated self-stress and self-driving forces; this will be treated in a future work. We assume that $\boldsymbol{\sigma}$ and s also depend on the same set of variables as ψ such that $\boldsymbol{\sigma}=\hat{\boldsymbol{\sigma}}(\boldsymbol{\varepsilon}^e)=\hat{\boldsymbol{\sigma}}(\boldsymbol{\varepsilon}-\boldsymbol{\varepsilon}^p,\theta)$ and $s=\hat{s}(\boldsymbol{\varepsilon}^e)=\hat{s}(\boldsymbol{\varepsilon}-\boldsymbol{\varepsilon}^p,\theta)$.

Let us assume that the initial state of $\mathcal{B}$ is characterized by $\boldsymbol{\alpha}_0(\boldsymbol{x})\neq\boldsymbol{0}$, $\boldsymbol{\varepsilon}_0^p(\boldsymbol{x})\neq\boldsymbol{0}$ and $s_0(\boldsymbol{x})\neq 0$ $\exists\boldsymbol{x}\in V$, and $\boldsymbol{\varepsilon}_0(\boldsymbol{x})=\boldsymbol{0}$ and $\theta(\boldsymbol{x})=\theta_0\neq 0,\forall\boldsymbol{x}\in V$. In this initial/reference state as well as any subsequent states, ψ must be positive. In the absence of dislocations and at zero deformation, we assume $\psi=\psi_0=0$. ψ should be independent of rigid body displacements. Recalling that we are in the case of small strains but large variations in θ are allowed, a simple expression for ψ that fulfills all these conditions is (Maitournam, 2017):

$$\rho\psi=\frac{1}{2}(\boldsymbol{\varepsilon}-\boldsymbol{\varepsilon}^p):\boldsymbol{\mathcal{C}}:(\boldsymbol{\varepsilon}-\boldsymbol{\varepsilon}^p)-\Delta\theta\boldsymbol{\beta}:(\boldsymbol{\varepsilon}-\boldsymbol{\varepsilon}^p)-\rho s_0\Delta\theta-\rho c_\varepsilon\theta\left(\ln\frac{\theta}{\theta_0}-1+\frac{\theta_0}{\theta}\right) \tag{3.45}$$

where $\boldsymbol{\mathcal{C}}$ is the fourth order elastic stiffness tensor, $\boldsymbol{\beta}=\boldsymbol{\mathcal{C}}:\boldsymbol{\gamma}$ is the second order thermal moduli tensor, c_ε is the specific heat capacity at constant strain and $\Delta\theta=\theta-\theta_0$. While deriving expression (3.45), it has been assumed that variations in $\boldsymbol{\mathcal{C}},\boldsymbol{\gamma},\rho$ and c_ε with respect to θ are negligible and these values are evaluated at $\boldsymbol{\varepsilon}_0(\boldsymbol{x})=\boldsymbol{0}$ and θ_0. From equations (3.42) and (3.43), and recalling the equations (3.6) and (3.8), we have the following constitutive laws:

$$\boldsymbol{\sigma}=\boldsymbol{\mathcal{C}}:\boldsymbol{\varepsilon}^e=\boldsymbol{\mathcal{C}}:\left(\boldsymbol{\varepsilon}-\boldsymbol{\varepsilon}^p-\boldsymbol{\varepsilon}^\theta\right)=\boldsymbol{\mathcal{C}}:(\boldsymbol{\varepsilon}-\boldsymbol{\varepsilon}^p)-\boldsymbol{\beta}\Delta\theta \tag{3.46}$$

$$s=s_0+\frac{1}{\rho}\boldsymbol{\beta}:(\boldsymbol{\varepsilon}-\boldsymbol{\varepsilon}^p)+c_\varepsilon\ln\frac{\theta}{\theta_0} \tag{3.47}$$

Equation (3.46) is the well-known Neumann-Duhamel's equation in thermoelasticity which reduces to the 3D Hooke's law under isothermal conditions at the reference temperature. Note that $\boldsymbol{\varepsilon}^p$ contains contributions from both $\boldsymbol{\varepsilon}^{p\parallel}$ and $\boldsymbol{\varepsilon}^{p\perp}$ and we have bypassed the Stokes-Helmholtz decomposition (3.10a) for $\boldsymbol{\varepsilon}^\theta$ by directly using the relationship (3.10b). Furthermore, we have also not attempted to obtain

an expression for s_0; it is more convenient to follow the evolution of $\Delta s = s - s_0 = \frac{1}{\rho}\boldsymbol{\beta}:(\boldsymbol{\varepsilon} - \boldsymbol{\varepsilon}^p) + c_\varepsilon \ln\frac{\theta}{\theta_0}$.

3.9 Dissipative constitutive relationships

Now, using equations (3.42) – (3.43) and neglecting $-\rho\frac{\partial\psi}{\partial\boldsymbol{a}}\cdot\dot{\boldsymbol{a}}$, inequality (3.41) reduces to the local dissipation inequality:

$$d = \boldsymbol{\sigma}:\dot{\boldsymbol{\varepsilon}}^p - \frac{1}{\theta}(\boldsymbol{q}\cdot\boldsymbol{\nabla}\theta) \geq 0 \tag{3.48}$$

which gives the global thermo-mechanical dissipation rate D:

$$D = \int_B \boldsymbol{\sigma}:\dot{\boldsymbol{\varepsilon}}^p dV - \int_B \frac{1}{\theta}(\boldsymbol{q}\cdot\boldsymbol{\nabla}\theta)dV \geq 0 \tag{3.49}$$

In order to derive the driving forces for dislocations, similar to the work of (Acharya, 2003), we shall work with the *global* thermo-mechanical dissipation. For the inequality (3.49) to be always satisfied, it is sufficient to independently satisfy $\int_B \boldsymbol{\sigma}:\dot{\boldsymbol{\varepsilon}}^p dV \geq 0$ and $\int_B \frac{1}{\theta}(\boldsymbol{q}\cdot\boldsymbol{\nabla}\theta)dV \leq 0$ at any given instant in time. There are infinite possible expressions for $\dot{\boldsymbol{\varepsilon}}^p$ and $\boldsymbol{q}$ that can respectively satisfy these conditions. For simplicity, we shall assume that $\dot{\boldsymbol{\varepsilon}}^p = \widehat{\dot{\boldsymbol{\varepsilon}}^p}(\boldsymbol{\sigma},\theta)$ and $\boldsymbol{q} = \widehat{\boldsymbol{q}}(\theta,\boldsymbol{\nabla}\theta,\boldsymbol{\varepsilon}-\boldsymbol{\varepsilon}^p)$.

Focusing on the first part of the dissipation inequality (3.49), it is well-known that $\dot{\boldsymbol{\varepsilon}}^p$ is non-linearly dependent on $\boldsymbol{\sigma}$ and θ. While the Clausius-Duhem inequality would allow dependence on additional variables, for the present purposes, only the dependence on $\boldsymbol{\sigma}$ and θ is considered. Note that due to the symmetry of the Cauchy stress tensor, we have $\int_B \boldsymbol{\sigma}:\dot{\boldsymbol{\varepsilon}}^p dV = \int_B \boldsymbol{\sigma}:\dot{\boldsymbol{U}}^p dV \geq 0$. Following (Acharya, 2003; Acharya and Roy, 2006), it can be shown that

$$\int_B \boldsymbol{\sigma}:\dot{\boldsymbol{U}}^p dV = \int_B \boldsymbol{\sigma}:\dot{\tilde{\boldsymbol{U}}}^p dV - \int_B \boldsymbol{W}_\sigma:\boldsymbol{S}^p dV \tag{3.50a}$$

where $\boldsymbol{W}_\sigma$ is such that it satisfies $\boldsymbol{\nabla}\times\boldsymbol{W}_\sigma = \boldsymbol{\sigma}^\perp$ where $\boldsymbol{\sigma}^\perp$ is the incompatible part of $\boldsymbol{\sigma}$. Using equation (3.30) we get:

$$\begin{aligned}\int_B \boldsymbol{\sigma}:\dot{\boldsymbol{U}}^p dV &= \int_B \textstyle\sum_\beta\left(\boldsymbol{\sigma}\cdot\boldsymbol{\alpha}^{p,\beta}\right):\mathbf{X}\cdot\boldsymbol{v}^{p,\beta}\, dV - \int_B \boldsymbol{W}_\sigma:\boldsymbol{S}^p dV \\ &= \int_B \textstyle\sum_\beta \boldsymbol{f}^{p,\beta}\cdot\boldsymbol{v}^{p,\beta}\, dV - \int_B \boldsymbol{W}_\sigma:\boldsymbol{S}^p dV \end{aligned} \tag{3.50b}$$

where $\boldsymbol{f}^{p,\beta} = \left(\boldsymbol{\sigma}\cdot\boldsymbol{\alpha}^{p,\beta}\right):\mathbf{X}$.

Focusing first on the second term on the right hand side of equation (3.50b), since we have to satisfy the condition (3.21), i.e. $\nabla\cdot\boldsymbol{\alpha}^p = \mathbf{0}$, we can deduce that $\boldsymbol{S}^p$ has to satisfy the constraint $\boldsymbol{\nabla}\cdot\boldsymbol{S}^p = \mathbf{0}$, which allows to define $\boldsymbol{S}^p = \sum_\beta \boldsymbol{S}^{p,\beta} = \boldsymbol{\nabla}\times\boldsymbol{\Omega}$, for a given $\boldsymbol{\Omega}$ (Acharya, 2003). Substituting this constraint in equation (3.50b) gives:

$$\int_B \boldsymbol{\sigma}:\dot{\boldsymbol{U}}^p dV = \int_B \textstyle\sum_\beta \boldsymbol{f}^{p,\beta}\cdot\boldsymbol{v}^{p,\beta}\, dV - \int_B \boldsymbol{\sigma}^\perp:\boldsymbol{\Omega}\, dV \tag{3.50c}$$

$\boldsymbol{\Omega}$ is interpreted as a nucleation rate (Acharya, 2004, 2003). Focusing now on the first term on the right-hand side of equation (3.50c) and substituting equation (3.22) in the expression for $\boldsymbol{f}^{p,\beta}$ we have:

$$\boldsymbol{f}^{p,\beta} = \frac{1}{V}\left(\boldsymbol{\sigma}\cdot\boldsymbol{b}^{p,\beta}\right)\times\boldsymbol{l}^{p,\beta} \tag{3.51}$$

Equation (3.51) is the well-known Peach-Koehler (PK) force used in dislocation dynamics simulations as the mechanical driving force for dislocation motion. $\boldsymbol{f}^{p,\beta}$ is also a function of θ through its dependence on $\boldsymbol{\sigma}$, $\boldsymbol{b}^{p,\beta}$ and $\boldsymbol{l}^{p,\beta}$. To ensure that inequality (3.50) is respected under all circumstances

(including presence/absence of $\boldsymbol{S}^p$), it is necessary that $\boldsymbol{f}^{p,\beta} \cdot \boldsymbol{v}^{p,\beta} \geq 0$ for each slip system β at every material point. The simplest way to ensure this is to assume the following linear relationship:

$$\boldsymbol{v}^{p,\beta} = \frac{1}{B^{p,\beta}} \boldsymbol{f}^{p,\beta} \tag{3.52}$$

where $B^{p,\beta} > 0$ is a material parameter, which is the inverse of the dislocation mobility and also depends on $\boldsymbol{\sigma}$ and θ (Olmsted et al., 2005). Equations (3.51) and (3.52) also include out-of-slip-plane components of the dislocation driving force and velocity, which are necessary to allow climb and cross-slip mechanisms as well as account for non-Schmid effects (Acharya, 2003).

If $\hat{\boldsymbol{n}}^\beta$ is the unit normal to the slip plane of the slip system β, then the glide $\boldsymbol{f}_g^\beta$, climb $\boldsymbol{f}_c^\beta$ and the normal to glide and climb $\boldsymbol{f}_n^\beta$ components of $\boldsymbol{f}^\beta$ are:

$$f_g^\beta(\boldsymbol{\sigma}, \theta) = \boldsymbol{f}^\beta(\boldsymbol{\sigma}, \theta) \cdot \frac{(\hat{\boldsymbol{n}}^\beta \times \boldsymbol{l}^\beta)}{|\hat{\boldsymbol{n}}^\beta \times \boldsymbol{l}^\beta|} \tag{3.53a}$$

$$f_c^\beta(\boldsymbol{\sigma}, \theta) = \boldsymbol{f}^\beta(\boldsymbol{\sigma}, \theta) \cdot \hat{\boldsymbol{n}}^\beta \tag{3.53b}$$

$$f_n^\beta(\boldsymbol{\sigma}, \theta) = \boldsymbol{f}^\beta(\boldsymbol{\sigma}, \theta) \cdot \frac{\boldsymbol{l}^\beta}{|\boldsymbol{l}^\beta|} \tag{3.53c}$$

Equations (3.53a), (3.53b) and (3.53c) account for both edge and screw dislocations. Dislocation velocity $\boldsymbol{v}^\beta$ can also be decomposed into glide $\boldsymbol{v}_g^\beta$, climb $\boldsymbol{v}_c^\beta$ and normal to glide and climb components $\boldsymbol{v}_n^\beta$. Decomposing the velocity into components requires adopting a non-linear crystal elasticity approach in order to represent individual dislocations with compact cores, i.e. to avoid unrealistic spread of the dislocation core, and capture the effects of Peierls stresses (Acharya, 2003; Zhang et al., 2015). Note that more complex relationships for each velocity component may become necessary at different θ; for example, different $B^\beta(\boldsymbol{\sigma}, \theta)$ can be used for the glide and climb velocity components. Furthermore, a distinction between the mobility $\left(1/B^\beta(\boldsymbol{\sigma}, \theta)\right)$ of edge and screw components (Zhu et al., 2013) and their dependence on temperature will also become important.

Focusing now on the second part of the dissipation inequality (3.49), i.e. $-\int_B \frac{1}{\theta}(\boldsymbol{q} \cdot \boldsymbol{\nabla}\theta) dV \geq 0$, the simplest relationship between $\boldsymbol{q}$ and $\boldsymbol{\nabla}\theta$ that satisfies this inequality over the entire volume as well as each material point individually is the well-known generalized Fourier law for heat conduction:

$$\boldsymbol{q}(\theta, \boldsymbol{\nabla}\theta, \boldsymbol{\varepsilon} - \boldsymbol{\varepsilon}^p) = -\boldsymbol{K}(\theta, \boldsymbol{\varepsilon} - \boldsymbol{\varepsilon}^p) \cdot \boldsymbol{\nabla}\theta \tag{3.54}$$

with the condition that the symmetric part of $\boldsymbol{K}$ is a positive definite tensor. Note that in the generalized Fourier law, $\boldsymbol{K}$ is dependent on both θ and $(\boldsymbol{\varepsilon} - \boldsymbol{\varepsilon}^p)$.

Coleman and Mizel (Coleman and Mizel, 1963) noteworthily viewed the Fourier law (3.54) as a limiting approximation, valid only for sufficiently homogeneous temperature fields, to a general nonlinear constitutive assumption for $\boldsymbol{q}$. Noting that $\boldsymbol{q}$ is more sensitive to $\boldsymbol{\nabla}\theta$ than any $\boldsymbol{\nabla}^n\theta$ ($n \geq 2$), they argued that a nonlinear constitutive assumption of $\boldsymbol{q}$ is more appropriate for a heterogeneous temperature distribution and provided corrections to the Fourier law involving a dependence on higher gradients of temperature.

3.10 Temperature rate

In order to obtain the temperature rate $\dot{\theta}$, we shall use equation (3.40) in the rate form of the Legendre transform of the internal energy density $u = \psi + \theta s$ to obtain:

$$\dot{u} = \dot{\psi} + s\dot{\theta} + \theta\dot{s} = \frac{1}{\rho}\boldsymbol{\sigma}: (\dot{\boldsymbol{\varepsilon}} - \dot{\boldsymbol{\varepsilon}}^p) + \theta\dot{s} \tag{3.55}$$

Next, in equation (3.55), we substitute $s = -\partial\psi/\partial\theta$ from equation (3.43), expand $\dot{\psi}$ via equation (3.40) while neglecting internal variables, and rearrange terms to get:

$$\rho\dot{u} = \boldsymbol{\sigma}:(\dot{\boldsymbol{\varepsilon}} - \dot{\boldsymbol{\varepsilon}}^p) + \theta\boldsymbol{\beta}:(\dot{\boldsymbol{\varepsilon}} - \dot{\boldsymbol{\varepsilon}}^p) + \rho c_\varepsilon\dot{\theta} \tag{3.56}$$

Inserting equation (3.56) into equation (3.35) gives:

$$\rho c_\varepsilon\dot{\theta} = \boldsymbol{\nabla}\cdot(\boldsymbol{K}\cdot\boldsymbol{\nabla}\theta) + \boldsymbol{\sigma}:\dot{\boldsymbol{\varepsilon}}^p - \theta\boldsymbol{\beta}:(\dot{\boldsymbol{\varepsilon}} - \dot{\boldsymbol{\varepsilon}}^p) + \rho r \tag{3.57}$$

Equation (3.57) complements equation (3.29) to show the intimate relationship between dislocation and thermal quasi-dislocation evolutions, and how one can act as a source/sink for the other. Note that due to the symmetry of $\boldsymbol{\sigma}$ and $\boldsymbol{\beta}$, we have $\boldsymbol{\sigma}:\dot{\boldsymbol{\varepsilon}}^p = \boldsymbol{\sigma}:\dot{\boldsymbol{U}}^p$ and $\boldsymbol{\beta}:(\dot{\boldsymbol{\varepsilon}} - \dot{\boldsymbol{\varepsilon}}^p) = \boldsymbol{\beta}:\left(\dot{\boldsymbol{U}} - \dot{\boldsymbol{U}}^p\right)$ with $\dot{\boldsymbol{U}}^p$ containing contributions from both $\dot{\boldsymbol{U}}^{p\parallel}$ and $\dot{\boldsymbol{U}}^{p\perp}$. This demonstrates that dislocation generation/annihilation/motion results in local temperature changes. If we consider steady-state heat conduction with no applied loading and non-evolving dislocations, then we have $\dot{\theta} = 0$. A deviation from this situation would result in $\dot{\theta} \neq 0$. For example, if the material is elastically loaded, i.e. dislocations remain stationary, then we get $\dot{\theta} \neq 0$ through the coupling term $\theta\boldsymbol{\beta}:\dot{\boldsymbol{\varepsilon}}$. If a stationary dislocation begins to move, say under an applied mechanical load, then its motion will also cause $\dot{\theta} \neq 0$. In turn, the temperature change would result in the evolution of the thermal quasi-dislocation density through the relationship for $\dot{\boldsymbol{\alpha}}^\theta$ presented in equation set (3.25).

Note that in the absence of plastic activity, equation (3.57) reduces to the well-known temperature rate equation in thermoelasticity, i.e. $\rho c_\varepsilon\dot{\theta} = \boldsymbol{\nabla}\cdot(\boldsymbol{K}\cdot\boldsymbol{\nabla}\theta) - \theta\boldsymbol{\beta}:\dot{\boldsymbol{\varepsilon}} + \rho r$.

3.11 Equation set for the geometrically linear T-FDM model

The final set of the most important field equations of the geometrically linear T-FDM problem are:

$$\begin{gathered}
\boldsymbol{\varepsilon}^\theta = \boldsymbol{\gamma}\Delta\theta \\
\dot{\boldsymbol{\alpha}}^{p,\beta} = -\boldsymbol{\nabla}\times\left(\boldsymbol{\alpha}^{p,\beta}\times\boldsymbol{v}^{p,\beta}\right) + \boldsymbol{S}^{p,\beta} \quad \text{and} \quad \boldsymbol{\alpha}^p = \textstyle\sum_\beta \boldsymbol{\alpha}^{p,\beta} \\
\dot{\boldsymbol{\alpha}}^\theta = (\boldsymbol{\nabla}\times\dot{\boldsymbol{\gamma}})\Delta\theta + (\boldsymbol{\nabla}\times\boldsymbol{\gamma})\dot{\theta} - \dot{\boldsymbol{\gamma}}\cdot[\boldsymbol{\nabla}(\Delta\theta)\cdot\mathbf{X}] - \boldsymbol{\gamma}\cdot\left[\boldsymbol{\nabla}(\dot{\Delta}\theta)\cdot\mathbf{X}\right] \\
\dot{\boldsymbol{\alpha}} = \dot{\boldsymbol{\alpha}}^\theta + \dot{\boldsymbol{\alpha}}^p \quad \text{and} \quad \boldsymbol{\alpha} = \boldsymbol{\nabla}\times\boldsymbol{U}^{e\perp} \\
\boldsymbol{\sigma} = \boldsymbol{C}:\boldsymbol{\varepsilon}^e = \boldsymbol{C}:(\boldsymbol{\varepsilon} - \boldsymbol{\varepsilon}^p) - \boldsymbol{\beta}\Delta\theta \\
\boldsymbol{q} = -\boldsymbol{K}\cdot\boldsymbol{\nabla}\theta \\
\boldsymbol{v}^{p,\beta} = \frac{1}{B^{p,\beta}}\boldsymbol{f}^{p,\beta} = \frac{1}{B^{p,\beta}}\left(\boldsymbol{\sigma}\cdot\boldsymbol{b}^{p,\beta}\right)\times\boldsymbol{l}^{p,\beta} \\
\rho\ddot{\boldsymbol{u}} = \boldsymbol{\nabla}\cdot\boldsymbol{\sigma} + \rho\boldsymbol{f}_v \\
\rho c_\varepsilon\dot{\theta} = \boldsymbol{\nabla}\cdot(\boldsymbol{K}\cdot\boldsymbol{\nabla}\theta) + \boldsymbol{\sigma}:\dot{\boldsymbol{\varepsilon}}^p - \theta\boldsymbol{\beta}:(\dot{\boldsymbol{\varepsilon}} - \dot{\boldsymbol{\varepsilon}}^p) + \rho r
\end{gathered} \tag{3.58}$$

3.12 Special cases of the T-FDM model

From the equation set (3.58) of the T-FDM model, it is possible to straightforwardly recover the equation sets for the conventional FDM, thermoelasticity, etc.

3.12.1 T-FDM with stationary dislocations

For a system subjected to mechanical loading and transient heat-flux/temperature boundary conditions without the motion of dislocations, i.e. $\dot{\tilde{\boldsymbol{U}}}^p = \mathbf{0}$, we have $\dot{\boldsymbol{U}}^{p\parallel} = \mathbf{0}$ but $\dot{\boldsymbol{\varepsilon}}^{p\perp} = sym\left(\dot{\boldsymbol{U}}^{p\perp}\right) \neq \mathbf{0}$ (see section 3.2). In this case, equation set (3.58) reduces to:

$$\begin{gathered}
\boldsymbol{\varepsilon}^\theta = \boldsymbol{\gamma}\Delta\theta \\
\dot{\boldsymbol{\alpha}}^{p,\beta} = \boldsymbol{S}^{p,\beta} \quad \text{and} \quad \boldsymbol{\alpha}^p = \textstyle\sum_\beta \boldsymbol{\alpha}^{p,\beta}
\end{gathered}$$

$$
\begin{gathered}
\dot{\boldsymbol{\alpha}}^{\theta} = (\boldsymbol{\nabla} \times \dot{\boldsymbol{\gamma}})\Delta\theta + (\boldsymbol{\nabla} \times \boldsymbol{\gamma})\dot{\theta} - \dot{\boldsymbol{\gamma}} \cdot [\boldsymbol{\nabla}(\Delta\theta) \cdot \mathbf{X}] - \boldsymbol{\gamma} \cdot \left[\boldsymbol{\nabla}(\dot{\Delta}\theta) \cdot \mathbf{X}\right] \\
\dot{\boldsymbol{\alpha}} = \dot{\boldsymbol{\alpha}}^{\theta} + \dot{\boldsymbol{\alpha}}^{p} \quad \text{and} \quad \boldsymbol{\alpha} = \boldsymbol{\nabla} \times \boldsymbol{U}^{e\perp} \\
\boldsymbol{\sigma} = \boldsymbol{\mathcal{C}}: \boldsymbol{\varepsilon}^{e} = \boldsymbol{\mathcal{C}}: (\boldsymbol{\varepsilon} - \boldsymbol{\varepsilon}^{p}) - \boldsymbol{\beta}\Delta\theta \\
\boldsymbol{q} = -\boldsymbol{K} \cdot \boldsymbol{\nabla}\theta \\
\rho\ddot{\boldsymbol{u}} = \boldsymbol{\nabla} \cdot \boldsymbol{\sigma} + \rho\boldsymbol{f}_{v} \\
\rho c_{\varepsilon}\dot{\theta} = \boldsymbol{\nabla} \cdot (\boldsymbol{K} \cdot \boldsymbol{\nabla}\theta) + \boldsymbol{\sigma}: \dot{\boldsymbol{\varepsilon}}^{p\perp} - \theta\boldsymbol{\beta}: (\dot{\boldsymbol{\varepsilon}} - \dot{\boldsymbol{\varepsilon}}^{p\perp}) + \rho r
\end{gathered}
\tag{3.59}
$$

3.12.2 T-FDM with stationary dislocations and steady-state heat conduction

For a system containing dislocations subjected to a steady-state heat-flux/temperature boundary condition without any mechanical loading such that the dislocations remain stationary, equation set (3.58) reduces to:

$$
\begin{gathered}
\boldsymbol{\varepsilon}^{\theta} = \boldsymbol{\gamma}\Delta\theta \\
\dot{\boldsymbol{\alpha}}^{p,\beta} = \mathbf{0} \quad \text{and} \quad \boldsymbol{\alpha}^{p} = \textstyle\sum_{\beta} \boldsymbol{\alpha}^{p,\beta} \\
\dot{\boldsymbol{\alpha}}^{\theta} = \mathbf{0} \\
\dot{\boldsymbol{\alpha}} = \mathbf{0} \quad \text{and} \quad \boldsymbol{\alpha} = \boldsymbol{\nabla} \times \boldsymbol{U}^{e\perp} \\
\boldsymbol{\sigma} = \boldsymbol{\mathcal{C}}: \boldsymbol{\varepsilon}^{e} = \boldsymbol{\mathcal{C}}: (\boldsymbol{\varepsilon} - \boldsymbol{\varepsilon}^{p}) - \boldsymbol{\beta}\Delta\theta \\
\boldsymbol{q} = -\boldsymbol{K} \cdot \boldsymbol{\nabla}\theta \\
\mathbf{0} = \boldsymbol{\nabla} \cdot \boldsymbol{\sigma} + \rho\boldsymbol{f}_{v}
\end{gathered}
\tag{3.60}
$$

3.12.3 FDM at reference temperature

In the case of an isothermal and adiabatic system at reference temperature, equation set (3.58) reduces to those of the geometrically linear FDM model.

$$
\begin{gathered}
\dot{\boldsymbol{\alpha}}^{p,\beta} = -\boldsymbol{\nabla} \times \left(\boldsymbol{\alpha}^{p,\beta} \times \boldsymbol{v}^{p,\beta}\right) \quad \text{and} \quad \boldsymbol{\alpha}^{p} = \textstyle\sum_{\beta} \boldsymbol{\alpha}^{p,\beta} \\
\dot{\boldsymbol{\alpha}} = \dot{\boldsymbol{\alpha}}^{p} \quad \text{and} \quad \boldsymbol{\alpha} = \boldsymbol{\nabla} \times \boldsymbol{U}^{e\perp} \\
\boldsymbol{\sigma} = \boldsymbol{\mathcal{C}}: \boldsymbol{\varepsilon}^{e} = \boldsymbol{\mathcal{C}}: (\boldsymbol{\varepsilon} - \boldsymbol{\varepsilon}^{p}) \\
\boldsymbol{v}^{p,\beta} = \frac{1}{B^{p,\beta}}\boldsymbol{f}^{p,\beta} = \frac{1}{B^{p,\beta}}\left(\boldsymbol{\sigma} \cdot \boldsymbol{b}^{p,\beta}\right) \times \boldsymbol{l}^{p,\beta} \\
\rho\ddot{\boldsymbol{u}} = \boldsymbol{\nabla} \cdot \boldsymbol{\sigma} + \rho\boldsymbol{f}_{v}
\end{gathered}
\tag{3.61}
$$

3.12.4 FDM at arbitrary constant temperature

In the case of an isothermal and adiabatic system at an arbitrary temperature, equation set (3.58) also reduces to those of the geometrically linear FDM model but with the coupling term in equation (3.46).

$$
\begin{gathered}
\boldsymbol{\varepsilon}^{\theta} = \boldsymbol{\gamma}\Delta\theta \\
\dot{\boldsymbol{\alpha}}^{p,\beta} = -\boldsymbol{\nabla} \times \left(\boldsymbol{\alpha}^{p,\beta} \times \boldsymbol{v}^{p,\beta}\right) \quad \text{and} \quad \boldsymbol{\alpha}^{p} = \textstyle\sum_{\beta} \boldsymbol{\alpha}^{p,\beta} \\
\dot{\boldsymbol{\alpha}} = \dot{\boldsymbol{\alpha}}^{p} \quad \text{and} \quad \boldsymbol{\alpha} = \boldsymbol{\nabla} \times \boldsymbol{U}^{e\perp} \\
\boldsymbol{\sigma} = \boldsymbol{\mathcal{C}}: \boldsymbol{\varepsilon}^{e} = \boldsymbol{\mathcal{C}}: (\boldsymbol{\varepsilon} - \boldsymbol{\varepsilon}^{p}) - \boldsymbol{\beta}\Delta\theta \\
\boldsymbol{v}^{p,\beta} = \frac{1}{B^{p,\beta}}\boldsymbol{f}^{p,\beta} = \frac{1}{B^{p,\beta}}\left(\boldsymbol{\sigma} \cdot \boldsymbol{b}^{p,\beta}\right) \times \boldsymbol{l}^{p,\beta} \\
\rho\ddot{\boldsymbol{u}} = \boldsymbol{\nabla} \cdot \boldsymbol{\sigma} + \rho\boldsymbol{f}_{v}
\end{gathered}
\tag{3.62}
$$

3.12.5 Fully-coupled thermoelasticity with thermal quasi-dislocations but no dislocations

In case of a system without dislocations, equation set (3.58) reduces to the following equation set:

$$
\begin{gathered}
\boldsymbol{\varepsilon}^{\theta} = \boldsymbol{\gamma}\Delta\theta \\
\dot{\boldsymbol{\alpha}}^{\theta} = (\boldsymbol{\nabla} \times \dot{\boldsymbol{\gamma}})\Delta\theta + (\boldsymbol{\nabla} \times \boldsymbol{\gamma})\dot{\theta} - \dot{\boldsymbol{\gamma}} \cdot [\boldsymbol{\nabla}(\Delta\theta) \cdot \mathbf{X}] - \boldsymbol{\gamma} \cdot \left[\boldsymbol{\nabla}(\dot{\Delta}\theta) \cdot \mathbf{X}\right]
\end{gathered}
$$

$$\dot{\boldsymbol{\alpha}} = \dot{\boldsymbol{\alpha}}^{\theta} \quad \text{and} \quad \boldsymbol{\alpha} = \boldsymbol{\nabla} \times \boldsymbol{U}^{e\perp}$$
$$\boldsymbol{\sigma} = \boldsymbol{C}: \boldsymbol{\varepsilon}^{e} = \boldsymbol{C}: \boldsymbol{\varepsilon} - \boldsymbol{\beta}\Delta\theta \tag{3.63}$$
$$\boldsymbol{q} = -\boldsymbol{K} \cdot \boldsymbol{\nabla}\theta$$
$$\rho\ddot{\boldsymbol{u}} = \boldsymbol{\nabla} \cdot \boldsymbol{\sigma} + \rho\boldsymbol{f}_{v}$$
$$\rho c_{\varepsilon}\dot{\theta} = \boldsymbol{\nabla} \cdot (\boldsymbol{K} \cdot \boldsymbol{\nabla}\theta) - \theta\boldsymbol{\beta}: \dot{\boldsymbol{\varepsilon}} + \rho r$$

4. Discussion and some illustrative examples

4.1 Implications of the adopted thermodynamics framework

4.1.1 Local thermodynamic equilibrium and the Clausius-Kelvin-Planck inequality under large thermal gradients

Since the T-FDM model is designed to study dislocation dynamics under large transient temperature gradients, such as those occurring due to solid-state thermal cycling during additive manufacturing, it is crucial to verify that local thermodynamic equilibrium is always respected under such conditions. Typically, the highest temperature rates occurring at a material point in a heat affected solid during an additive manufacturing process are of the order of $10^6\ K/s$, i.e. $10^{-6}\ K/picosecond$. Atomic fluctuations that accommodate thermal changes typically do so in timespans of $10^{-2} - 1\ picoseconds$. Therefore, we can safely assume that even for the highest temperature rates occurring during additive manufacturing, thermal changes are instantaneously accommodated via atomic fluctuations. In other words, thermal equilibrium can be assumed to exist at each material point in the system at any given instant in time. Furthermore, the thermal stresses generated (if any) due to the temperature gradients are also equilibrated rapidly resulting in a mechanical equilibrium at each material point. For now, we will assume that under such large temperature changes, a material point does not have sufficient time to change its chemical configuration; chemical changes due to temperature changes shall be addressed in a future work. The combined effect of these considerations is that for a system subjected to $10^6\ K/s$, local thermodynamic equilibrium can be assumed everywhere in the system at any given instant in time.

The Clausius-Kelvin-Planck inequality and the local thermodynamic equilibrium conditions impose an upper limit on the magnitudes of transient temperature gradients that can be induced under the action of temperature and heat flux boundary conditions. For local thermodynamic equilibrium to be valid, each material point in the system should be able to adjust to the induced thermal and mechanical changes in a timespan that is negligibly small in comparison to the timespan over which the boundary conditions evolve. Indeed, this will be the case when T-FDM is applied to study dislocation dynamics due to solid-state thermal cycling during additive manufacturing.

4.1.2 Definition of temperature

As noted by Lebon et al. (Lebon et al., 2008), in most RT based dislocation mechanics models, entropy and temperature are taken as primitive undefined entities whose physical meaning is often unclear. In fact, during the development of the T-FDM model, an empirical temperature scale was not defined but it was assumed to exist. While an undefined temperature is not a significant cause for concern under isothermal and adiabatic conditions, it cannot be ignored when considering large temperature changes.

In section 4.1.1, we argued that local thermodynamic equilibrium was admissible for the range of problems that will be tackled by the T-FDM model. Based on this assumption, we can use the equilibrium definition of absolute temperature. This requires redefining the dependent variables for entropy s. From equations (3.42) and (3.43), we can construct the following differential expression for ψ

$$\mathrm{d}\psi = -s\mathrm{d}\theta + \frac{1}{\rho}\boldsymbol{\sigma}: \mathrm{d}(\boldsymbol{\varepsilon} - \boldsymbol{\varepsilon}^{p}) \tag{4.1}$$

Using its Legendre transform $\psi = u - \theta s$, equation (4.1) can also be written as

$$\mathrm{d}s = \frac{1}{\theta}\mathrm{d}u - \frac{1}{\rho\theta}\boldsymbol{\sigma}:\mathrm{d}(\boldsymbol{\varepsilon} - \boldsymbol{\varepsilon}^p) \tag{4.2}$$

Equation (4.2) is the Gibbs equation for our thermo-elasto-plastic problem, which also implies that $s = \hat{s}(\boldsymbol{\varepsilon} - \boldsymbol{\varepsilon}^p, u)$. Then, we get the following definition of θ:

$$\frac{1}{\theta} = \left.\frac{\partial s}{\partial u}\right|_{\boldsymbol{\varepsilon}-\boldsymbol{\varepsilon}^p\,=\,constant} \tag{4.3}$$

In order for the above definition of temperature to be valid in thermal equilibrium, it is necessary to augment the above equation as follows:

$$\frac{1}{\theta} = \left.\frac{\partial s}{\partial u}\right|_{\boldsymbol{\varepsilon}-\boldsymbol{\varepsilon}^p\,=\,constant,\boldsymbol{q}=0} = \frac{1}{T} \tag{4.4}$$

where T is the equilibrium measure of θ.

In this work, by assuming local thermodynamic equilibrium, we have assumed that the temperature distribution is uniform within a subdomain volume represented by a material point in the body. In other words, there are no temperature gradients present within the subdomain even though there may be strong temperature gradients present in the entire system. Therefore, we can use the equilibrium definition of temperature equation (4.2) for the range of applicability of the T-FDM model.

4.1.3 Definition of entropy

While the existence of entropy as a state function has been proven (Coleman et al., 1981; Coleman and Owen, 1974; Serrin, 1979), however, there is no consensus on its unambiguous definition. At the level of continuum mechanics, an expression for entropy is often obtained from an assumed expression for the free energy potential; for example, see expression (3.47) and its derivation. However, any such expression for entropy is non-unique. In fact, there are infinite different expressions of entropy that can satisfy the Clausius-Duhem inequality (Coleman et al., 1981; Meixner, 1973).

A noteworthy contribution was made by Acharya (Acharya, 2011) who developed an expression for the entropy of an isolated constrained ergodic Hamiltonian system and demonstrated that it is related to the continuum definition of the specific entropy field. At the continuum level, the approach allows for the evolution of the energy field (via the energy balance equation (3.35)) and it assumes that during each short time interval (from the perspective of a slow time scale during which local equilibrium can be assumed to be instantaneously achieved), the local energy at each material point remains constant. During this short interval in time, the underlying ensemble of atoms can be assumed to be a constrained microcanonical ensemble with a constant energy, which allows one to define the entropy from a statistical mechanics standpoint. Once the local energy and entropy are known, the temperature field can be obtained via eqn. (4.4). Acharya (Acharya, 2011) applied these developments to a spatially and temporally averaged version of FDM. The statistical mechanics based definition of entropy by Acharya (Acharya, 2011) and its connection to the continuum definition of entropy can also be applied to this work.

4.2 Some illustrative examples

Let us consider a rectangular parallelepiped domain $\mathcal{B}$ with homogeneous isotropic linear elastic and thermal properties (λ, μ – Lamé constants, γ – coefficient of thermal expansion, $k -$ thermal conductivity) to be in thermal equilibrium with its surroundings at θ_0. All material properties are defined at θ_0 and assumed to be constant with respect to temperature and strain rates. Let the body have dimensions $[-H, H]$, $[-L, L]$ and $[-W, W]$ along $\hat{e}_1$, $\hat{e}_2$ and $\hat{e}_3$ directions, respectively.

4.2.1 Thermal quasi-dislocations due to steady-state heat conduction in an elastic medium without dislocations

Unconstrained system: Traction-free boundary conditions are imposed everywhere on $\partial\mathcal{B}$. The surface normal to $+\hat{e}_2$ is subjected to θ^h $\left(\theta_{solidus} > \theta^h > \theta_0\right)$ and the surface normal to $-\hat{e}_2$ is kept at θ_0. Since we are using the Fourier's law of heat conduction (equation (3.54)), a heat-flux $\boldsymbol{q} = -q\hat{e}_2 = -\frac{(\theta^h-\theta_0)}{2L}\hat{e}_2 = -k\theta_{,2}\hat{e}_2$ $\left(\text{with } \theta_{,2} = \frac{q}{k} = constant > 0 \text{ and } k > 0\right)$ is *instantaneously* generated everywhere in the body resulting in a steady-state heat conduction. This results in the generation of a linear temperature profile through the body, which satisfies equation (3.57). This temperature field induces thermal strains, which are assumed to be spherically symmetric such that $\varepsilon_{11}^{\theta} = \varepsilon_{22}^{\theta} = \varepsilon_{33}^{\theta} = \gamma(\theta - \theta_0) = \gamma\Delta\theta$.

Next, we consider the Beltrami-Mitchell compatibility condition for our traction free boundary condition problem:

$$\sigma_{ij,kk} + \frac{1}{1+\nu}\sigma_{kk,ij} = 0 \tag{4.5}$$

The only statically admissible $\boldsymbol{\sigma}$ that satisfies condition (4.5) is $\boldsymbol{\sigma} = \boldsymbol{\mathcal{C}}:\boldsymbol{\varepsilon}^e = \boldsymbol{\mathcal{C}}:\left(\boldsymbol{\varepsilon} - \boldsymbol{\varepsilon}^{\theta}\right) = \mathbf{0}$. Therefore, we have $\boldsymbol{\varepsilon}^e = \mathbf{0}$, and by consequence, $\boldsymbol{\varepsilon} = \boldsymbol{\varepsilon}^{\theta}$.

Note that the temperature field will induce thermal quasi-dislocations with the only non-zero components of $\boldsymbol{\alpha}^{\theta}$ being $\alpha_{13}^{\theta} = \gamma\frac{q}{k}$ and $\alpha_{31}^{\theta} = -\gamma\frac{q}{k}$. Since there are no dislocations present in the body and there is no history of dislocation motion, we have $\boldsymbol{U}^{p\perp} = \mathbf{0}$, $\boldsymbol{U}^{p\parallel} = \mathbf{0}$ and $\boldsymbol{\alpha}^p = \mathbf{0}$. Therefore, $\boldsymbol{\alpha} = \boldsymbol{\alpha}^{\theta}$ and the only non-zero components of $\boldsymbol{\alpha}$ are $\alpha_{13} = \alpha_{13}^{\theta} = \gamma\frac{q}{k}$ and $\alpha_{31} = \alpha_{31}^{\theta} = -\gamma\frac{q}{k}$.

From equation (3.14), we have $\boldsymbol{\alpha} = \boldsymbol{\nabla} \times \boldsymbol{U}^e = \boldsymbol{\nabla} \times \boldsymbol{U}^{e\perp}$. However, with $\boldsymbol{\varepsilon}^e = \mathbf{0}$ and $\boldsymbol{\alpha} = \boldsymbol{\alpha}^{\theta} \neq \mathbf{0}$, $\boldsymbol{U}^e$ has to be anti-symmetric and not equal to $\mathbf{0}$. The anti-symmetric part of $\boldsymbol{U}^e$ is also known as the second order elastic rotation tensor and we shall denote it by $\boldsymbol{\omega}^e$. Therefore, we have $\boldsymbol{\alpha} = \boldsymbol{\nabla} \times \boldsymbol{\omega}^e \neq \mathbf{0}$. Note that lack of dislocations and no history of dislocation motion implies that the plastic rotation tensor $\boldsymbol{\omega}^p = \mathbf{0}$, and since thermal strains are symmetric tensors, we end up with the total rotation tensor $\boldsymbol{\omega} = \boldsymbol{\omega}^e$ and $\boldsymbol{\alpha} = \boldsymbol{\nabla} \times \boldsymbol{\omega} \neq \mathbf{0}$. Next, following the convention adopted in (Upadhyay et al., 2013), we relate $\boldsymbol{\omega}$ and $\boldsymbol{\omega}^e$ to total and elastic rotation vectors, say $\boldsymbol{w}$ and $\boldsymbol{w}^e$, respectively, as $\omega_{ij} = -e_{ijk}w_k$ and $\omega_{ij}^e = -e_{ijk}w_k^e$. Consequently, $\alpha_{ij} = \delta_{ij}w_{k,k}^e - w_{j,i}^e = \delta_{ij}w_{k,k} - w_{j,i}$. From here, we get $w_{1,3}^e = w_{1,3} = \gamma\frac{q}{k}$ and $w_{3,1}^e = w_{3,1} = -\gamma\frac{q}{k}$; note that we can also define an elastic rotation vector whose only non-zero components will also satisfy these expressions. We can define second order elastic and total curvature tensors as $\boldsymbol{\kappa}^e = \boldsymbol{\kappa}^{e\parallel} = \boldsymbol{\nabla}\boldsymbol{w}^e$ and $\boldsymbol{\kappa} = \boldsymbol{\kappa}^{\parallel} = \boldsymbol{\nabla}\boldsymbol{w}$, respectively (Upadhyay et al., 2013). For the current problem, we have $\kappa_{13}^e = \kappa_{13} = \gamma\frac{q}{k}$ and $\kappa_{31}^e = \kappa_{31} = -\gamma\frac{q}{k}$. Finally, for the adopted convention, $\boldsymbol{w}$ is related to $\boldsymbol{u}$ as $\boldsymbol{w} = \frac{\mathbf{1}}{\mathbf{2}}\boldsymbol{\nabla} \times \boldsymbol{u}$, which gives $u_{3,23} - u_{2,33} = 2\gamma\frac{q}{k}$ and $u_{1,21} - u_{2,11} = 2\gamma\frac{q}{k}$; these equations complement the ones obtained from equation (4.5) after introducing equation (3.46) in it.

The above analysis highlights that when a stress-free and dislocation-free isotropic linear elastic system is subjected to steady-state heat conduction, thermal quasi-dislocations are generated and they induce constant elastic and total curvature fields, linearly varying elastic and total rotation fields and quadratically varying total displacement field in $\mathcal{B}$.

Partly constrained: We now consider the case where $\mathcal{B}$ is placed inside a hollow rigid cylinder (with a rectangular cross-section), which is a perfect insulator, such that $u_1 = u_3 = 0$ is imposed on the surfaces of $\mathcal{B}$ normal to $\pm\hat{e}_1$ and $\pm\hat{e}_3$. We also assume that $\mathcal{B}$ is in perfect frictionless contact with the inside walls of this cylinder. We continue to assume $\mathcal{B}$ is subjected to traction-free boundary condition on the surfaces normal to $\pm\hat{e}_2$. Similar to the previous case, let $\mathcal{B}$ be instantaneously subjected to θ^h on $+\hat{e}_2$ such that a constant heat-flux of $\boldsymbol{q} = -q\hat{e}_2$, a thermal gradient $\theta_{,2} = \frac{q}{k} = \text{constant}$, and spherically symmetric thermal

strains $\varepsilon_{11}^{\theta} = \varepsilon_{22}^{\theta} = \varepsilon_{33}^{\theta} = \gamma(\theta - \theta_0) = \gamma\Delta\theta$ are generated. We have $u_2 \neq 0$ and $\varepsilon_{22} = \varepsilon_{22}^{\theta}$. All other components of $\boldsymbol{u}$ and $\boldsymbol{\varepsilon}$ are equal to 0. We now have, $\varepsilon_{11}^{e} = -\varepsilon_{11}^{\theta} = \varepsilon_{33}^{e} = -\varepsilon_{33}^{\theta} = -\gamma\Delta\theta$ and the remaining components of $\boldsymbol{\varepsilon}^e$ are equal to zero. Based on the above conditions, the only non-zero components of the statically admissible $\boldsymbol{\sigma}$ are $\sigma_{11} = \sigma_{33} = -(3\lambda + 2\mu)\gamma\Delta\theta$, which satisfy the equilibrium equation. We also note that geometrical constraints impose $\boldsymbol{w} = \boldsymbol{w}^e = \boldsymbol{0}$ and consequently, $\boldsymbol{\omega}^e = \boldsymbol{0}$. No dislocations as well as no history of dislocation motion implies $\boldsymbol{U}^{p\perp} = \boldsymbol{0}$ and $\boldsymbol{U}^{p\parallel} = \boldsymbol{0}$, respectively, together with $\boldsymbol{w}^p = \boldsymbol{0}$.

Now, from equation (3.10b), we get $\boldsymbol{\alpha}^{\theta} = -\boldsymbol{\nabla} \times \boldsymbol{\varepsilon}^{\theta} = -\boldsymbol{\nabla} \times \boldsymbol{U}^{\theta\perp} \neq \boldsymbol{0}$. The only non-zero components of $\boldsymbol{\alpha}^{\theta}$ are $\alpha_{13}^{\theta} = \varepsilon_{11,2}^{\theta} = \gamma\frac{q}{k}$ and $\alpha_{31}^{\theta} = -\varepsilon_{33,2}^{\theta} = -\gamma\frac{q}{k}$. Next, from equation set (3.19), we have $\boldsymbol{\alpha} = \boldsymbol{\nabla} \times \boldsymbol{\varepsilon}^e = \boldsymbol{\alpha}^{\theta}$. The only non-zero components of $\boldsymbol{\alpha}$ are $\alpha_{13} = -\varepsilon_{11,2}^{e\perp} = \alpha_{13}^{\theta} = \gamma\frac{q}{k}$ and $\alpha_{31} = \varepsilon_{33,2}^{e\perp} = \alpha_{31}^{\theta} = -\gamma\frac{q}{k}$. From here, we obtain $\varepsilon_{11}^{e\perp} = -\gamma\Delta\theta = -\varepsilon_{11}^{\theta}$ and $\varepsilon_{33}^{e\perp} = -\gamma\Delta\theta = -\varepsilon_{33}^{\theta}$, which are exact up to a gradient term. From equation (3.46), we obtain,

$$\sigma_{11} = -(3\lambda + 2\mu)\gamma\Delta\theta \qquad \text{and} \qquad \sigma_{33} = -(3\lambda + 2\mu)\gamma\Delta\theta \tag{4.6}$$

These equations imply that thermal quasi-dislocations and thermal stresses are generated in an isotropic linear elastic body with steady-state heat conduction when it is subjected to external constraints. Note that this problem is an example of a thermoelastic problem.

Let us now imagine that the body contains dislocations of the kind $\alpha_{13} = \alpha_{13}^{p} = \gamma\frac{q}{k}$ and $\alpha_{31} = \alpha_{31}^{p} = -\gamma\frac{q}{k}$ under isothermal conditions at θ_0. In this case, we have two edge dislocations everywhere in the domain. The first one could have its Burgers and line vectors along directions $\hat{e}_1$ and $\hat{e}_3$ (or $-\hat{e}_1$ and $-\hat{e}_3$), respectively. The second one could have its Burgers and line vectors along directions $-\hat{e}_3$ and $\hat{e}_1$ (or $\hat{e}_3$ and $-\hat{e}_1$), respectively. Indeed, their presence would be associated with additional components of $\boldsymbol{U}^{e\perp} = -\boldsymbol{U}^{p\perp} \neq \boldsymbol{0}$ and possibly $\boldsymbol{\sigma} \neq \boldsymbol{0}$. Furthermore, the presence of dislocations also induces incompatible elastic and plastic rotations, which result in the formation of compatible elastic and plastic curvatures $\boldsymbol{\kappa}^{e\parallel} = \boldsymbol{\nabla}\boldsymbol{w}^{e\perp}$ and $\boldsymbol{\kappa}^{p\parallel} = \boldsymbol{\nabla}\boldsymbol{w}^{p\perp} = -\boldsymbol{\kappa}^{e\parallel}$, respectively (Upadhyay et al., 2013). All these fields will have non-zero gradients. This consideration demonstrates that thermal quasi-dislocations arising from a linear temperature profile under a steady-state condition cannot be transformed into dislocations under these conditions.

A comparison of the unconstrained and partly constrained cases studied in this section reveals that in the former case thermal quasi-dislocations induce elastic and total rotation fields but no stresses and in the latter case they induce stresses but no rotation fields. However, in a different partly constrained case, thermal quasi-dislocations may additionally induce rotation fields.

4.2.2 A stationary screw dislocation during steady-state heat conduction

Let us consider the case of a straight screw dislocation in our isotropic linear elastic body $\mathcal{B}$ at θ_0. Let the screw dislocation have a Burgers vector $\boldsymbol{b}^p(\theta_0) = b\hat{e}_3$ and line vector $\boldsymbol{l}^p(\theta_0) = l\hat{e}_3$. The only non-zero component of $\boldsymbol{\alpha}^p$ is $\boldsymbol{\alpha}^p(\theta_0) = \alpha_{33}^p(\theta_0)\hat{e}_3 \otimes \hat{e}_3$. We shall assume that $\mathcal{B}$ is long enough along directions $\hat{e}_1$ and $\hat{e}_2$ so that we can impose traction free boundary conditions on the surfaces normal to $\pm\hat{e}_1$ and $\pm\hat{e}_2$ without any significant impact on the stress field near the dislocation. We shall assume that periodic boundary conditions on surfaces of $\mathcal{B}$ normal to $\pm\hat{e}_3$.

Following (Acharya, 2001), we define

$$\alpha_{33}^p = \begin{cases} \frac{b}{\pi r_c}\left(\frac{1}{r} - \frac{1}{r_c}\right) & ; r < r_c \\ 0 & ; r \geq r_c \end{cases} \tag{4.7}$$

where $r = \sqrt{x_1^2 + x_2^2}$ and r_c defines the limit of the dislocation "core" region. Note that α_{33}^p does not vary along the z-axis. In the presence of this screw dislocation under isothermal conditions at θ_0, we have $\boldsymbol{U}^{in} =$

$\boldsymbol{U}^{p\perp} = -\boldsymbol{U}^{e\perp}$. The only two non-zero components of $\boldsymbol{U}^{e\perp}$ are $U_{31}^{e\perp}$ and $U_{32}^{e\perp}$. Using the Riemann-Graves integral operator, Acharya (Acharya, 2001) derived the following expressions for $U_{31}^{e\perp}$ and $U_{32}^{e\perp}$:

$$\left.\begin{aligned} U_{31}^{e\perp} = -U_{31}^{p\perp} &= \begin{cases} -\frac{b}{\pi r_c}\frac{x_2}{r^2}\left(r - \frac{r^2}{2r_c}\right) & ; r < r_c \\ -\frac{b}{2\pi}\frac{x_2}{r^2} & ; r \geq r_c \end{cases} \\ U_{32}^{e\perp} = -U_{32}^{p\perp} &= \begin{cases} \frac{b}{\pi r_c}\frac{x_1}{r^2}\left(r - \frac{r^2}{2r_c}\right) & ; r < r_c \\ \frac{b}{2\pi}\frac{x_1}{r^2} & ; r \geq r_c \end{cases} \end{aligned}\right\} \tag{4.8}$$

If we use the following form of the elastic constitutive law $\boldsymbol{\sigma} = \boldsymbol{\mathcal{C}}:\left(\boldsymbol{U} - \boldsymbol{U}^{in}\right)$ and neglect body forces, then the equilibrium equation $\boldsymbol{\nabla} \cdot \boldsymbol{\sigma} = \boldsymbol{0}$ becomes

$$c_{ijkl}u_{k,lj} = f_i \tag{4.9}$$

where $f_i = c_{imnp}U_{np,m}^{in}$. Following (Berbenni et al., 2014), this equation can be solved in the Fourier space to obtain an expression of the displacement field, and eventually the stress field, as a function of $\boldsymbol{U}^{in}$:

$$\boldsymbol{\sigma}(\boldsymbol{x}) = \begin{cases} \mathcal{F}^{-1}\left[\left(\mathcal{C}_{ijkl}\hat{\Gamma}_{klmn}(\boldsymbol{\xi})\mathcal{C}_{mnpq} - \mathcal{C}_{ijpq}\right)\hat{U}_{pq}^{in}(\boldsymbol{\xi})\right] & ; \boldsymbol{\xi} \neq \boldsymbol{0} \\ \boldsymbol{\Sigma} & ; \boldsymbol{\xi} = \boldsymbol{0} \end{cases} \tag{4.10}$$

where an overhead hat implies the Fourier transform of a variable, $\mathcal{F}^{-1}$ is the inverse Fourier transform operator, $\boldsymbol{\xi}$ is a vector in Fourier space, $\boldsymbol{\Sigma} = \langle\boldsymbol{\sigma}\rangle$ is the volume averaged stress field that corresponds to the zeroth frequency $\boldsymbol{\xi} = \boldsymbol{0}$ in the Fourier space, $\mathcal{C}_{ijkl} = \lambda\delta_{ij}\delta_{kl} + \mu\left(\delta_{ik}\delta_{jl} + \delta_{il}\delta_{jk}\right)$ for an isotropic elastic material, and $\hat{\Gamma}_{klmn}(\boldsymbol{\xi})$ is the modified Green's operator whose expression for the isotropic linear elastic case is given as:

$$\hat{\Gamma}_{klmn}(\boldsymbol{\xi}) = \frac{1}{2\mu\xi^2}\left(\delta_{km}\xi_n\xi_l + \delta_{kn}\xi_m\xi_l + \delta_{lm}\xi_k\xi_n + \delta_{ln}\xi_k\xi_m\right) - \frac{\lambda+\mu}{\mu(\lambda+2\mu)}\frac{\xi_k\xi_l\xi_m\xi_n}{\xi^4} \tag{4.11}$$

Equation (4.10) could have also been used to deduce the relationship (4.6); noting that a multiplication with $\xi_i\xi_j$ in Fourier space corresponds to partial derivatives with respect to x_i and x_j in real space, it is straightforward to obtain equation (4.6) from equation (4.10) for the linearly varying thermal strain components.

For our stationary screw dislocation problem under isothermal conditions, it can be shown that the only non-zero components of the equilibrated $\boldsymbol{\sigma}$ are $\sigma_{31} = \sigma_{13}$ and $\sigma_{32} = \sigma_{23}$, and they are trivially related to $-U_{31}^{in} = U_{31}^{e\perp} = \mathcal{F}^{-1}\left[\hat{U}_{31}^{e\perp}\right]$ and $-U_{32}^{in} = U_{32}^{e\perp} = \mathcal{F}^{-1}\left[\hat{U}_{32}^{e\perp}\right]$, respectively, as

$$\begin{aligned} \sigma_{31} = \sigma_{13} = \mu U_{31}^{e\perp} \\ \sigma_{32} = \sigma_{23} = \mu U_{32}^{e\perp} \end{aligned} \tag{4.12}$$

We can deduce from equation (4.8) that $\langle U_{31}^{e\perp}\rangle = \langle U_{32}^{e\perp}\rangle = 0$; where $\langle\ \ \rangle$ represents a sum over the volume. Furthermore, the surfaces normal to $\pm\hat{e}_3$ at infinity will experience a non-zero distribution of σ_{13} and σ_{23} whose sum over these surfaces will be zero because $\langle U_{31}^{e\perp}\rangle_S = \langle U_{32}^{e\perp}\rangle_S = 0$; where $\langle\ \ \rangle_S$ represents a sum over a surface.

The screw dislocation will also induce elastic (and plastic) rotation field with components $w_1^e = \frac{1}{2}U_{32}^{e\perp}$ and $w_2^e = \frac{1}{2}U_{31}^{e\perp}$ together with plastic rotations $\boldsymbol{w}^p = -\boldsymbol{w}^e$. These will result in elastic curvature components $\kappa_{11}^{e\parallel} = \frac{1}{2}U_{32,1}^{e\perp}$, $\kappa_{12}^{e\parallel} = \frac{1}{2}U_{32,2}^{e\perp}$, $\kappa_{21}^{e\parallel} = \frac{1}{2}U_{31,1}^{e\perp}$ and $\kappa_{22}^{e\parallel} = \frac{1}{2}U_{31,2}^{e\perp}$ together with plastic curvatures $\boldsymbol{\kappa}^p = -\boldsymbol{\kappa}^e$; note that both $\boldsymbol{\kappa}^e$ and $\boldsymbol{\kappa}^p$ vary non-linearly in space.

Next, we impose the same temperature and heat-flux boundary conditions as done in section 4.2.1 to obtain a constant temperature gradient $\theta_{,2} = \frac{q}{k} = \frac{\theta^h - \theta_0}{2L}$ such that the dislocation line experiences the same temperature $\theta^* > \theta_0$ everywhere along the line. This results in an increase in the Burgers vector magnitude $b^* > b$ as well as the line vector magnitude $l^* > l$. The dislocation density α_{33}^p also increases (equation (4.7)) to α_{33}^{p*} (say) and the dislocation core spreads $r_0^* > r_0$. This affects the magnitudes of $U_{31}^{e\perp}$ and $U_{32}^{e\perp}$ (equation (4.8)), which in turn affect the magnitudes of σ_{13} and σ_{23} (equation (4.12)), respectively.

Similar to the cases in section 4.2.1, thermal strains $\varepsilon_{11}^\theta = \varepsilon_{22}^\theta = \varepsilon_{33}^\theta = \gamma(\theta - \theta_0) = \gamma\Delta\theta$ and thermal quasi-dislocations $\alpha_{13}^\theta = \gamma\frac{q}{k}$ and $\alpha_{31}^\theta = -\gamma\frac{q}{k}$ are generated. However, unlike the cases from section 4.2.1, a screw dislocation is now present in the domain, which results in the Nye's tensor $\boldsymbol{\alpha} = \boldsymbol{\alpha}^p + \boldsymbol{\alpha}^\theta = \alpha_{13}^\theta \hat{e}_1 \otimes \hat{e}_3 + \alpha_{31}^\theta \hat{e}_3 \otimes \hat{e}_1 + \alpha_{33}^{p*} \hat{e}_3 \otimes \hat{e}_3$. From equation (3.14), we obtain $U_{33,2}^{e\perp} - U_{32,3}^{e\perp} = \alpha_{31}$, $U_{12,1}^{e\perp} - U_{11,2}^{e\perp} = \alpha_{13}$ and $U_{32,1}^{e\perp} - U_{31,2}^{e\perp} = \alpha_{33}$. The first two expressions are solely due to the temperature field and the last expression is solely due to the screw dislocation; note that the second term in the first expression, i.e. $-U_{32,3}^{e\perp}$, has to be solely due to the temperature field because the screw dislocation is infinitely long along direction $\hat{e}_3$ and the distortion fields induced by it do not vary along that direction. From the first case in section 4.2.1, we know that these thermal quasi-dislocations will induce $\kappa_{13}^e = \kappa_{13} = \gamma\frac{q}{k}$ and $\kappa_{31}^e = \kappa_{31} = -\gamma\frac{q}{k}$. The combined elastic curvature field from the screw dislocation and thermal quasi-dislocations has six non-zero terms: κ_{11}, κ_{12}, κ_{13}, κ_{21}, κ_{22} and κ_{31}. Note that κ_{13}^e arises from the elastic rotation w_1^e, which varies along $\hat{e}_3$.

Similar to the first case in section 4.2.1, thermal quasi-dislocations will not induce any stresses. Note that while a distribution of σ_{13} and σ_{23} exists on the surfaces normal to $\pm\hat{e}_3$ at infinity due to the presence of the screw dislocation, however, these stress components do not impede the volume expansion of the body. Therefore, the only statically admissible stress field will be the one having σ_{13} and σ_{23} as the only non-zero components.

4.2.3 A moving screw dislocation inducing a transient temperature change

Let us reconsider the case of the screw dislocation from section 4.2.2 with $\boldsymbol{b}^p(\theta_0) = b_0\hat{e}_3$, $\boldsymbol{l}^p(\theta_0) = l_0'\hat{e}_3$ and $\boldsymbol{\alpha}^p(\theta_0) = \alpha_{33}^p(\theta_0)\hat{e}_3 \otimes \hat{e}_3$, with $\alpha_{33}^p(\theta_0) = b_0 l_0'$ given by equation (4.7), in a rectangular parallelepiped body $\mathcal{B}$ with surface $\partial\mathcal{B}$ having a uniform temperature θ_0 everywhere. Periodic boundary conditions are imposed on surfaces of $\mathcal{B}$ along $\pm\hat{e}_3$ and we assume that there is no variation of any variable along $\pm\hat{e}_3$. In the initial state, let the screw dislocation be located at $(x_1, x_2) \equiv (0,0)$. $\mathcal{B}$ has dimensions $(-H, H)$ along $\hat{e}_1$ and $(-L, L)$ along $\hat{e}_2$. Dirichlet temperature boundary conditions $\theta(-H, x_2, t) = \theta(H, x_2, t) = \theta(x_1, -L, t) = \theta(x_1, L, t) = \theta_0$ are imposed. Traction-free boundary conditions are imposed on portions of $\partial\mathcal{B}$ with the normal parallel to $\pm\hat{e}_2$. The portion of $\partial\mathcal{B}$ with the normal parallel to $-\hat{e}_1$ is fixed. We assume that the body $\mathcal{B}$ is long enough along directions $\hat{e}_1$ and $\hat{e}_2$ so that these boundary conditions have a negligible impact on the stresses (σ_{13} and σ_{23}) generated by the dislocation.

At $t = 0$, we impose a constant shear stress τ along direction $-\hat{e}_3$ on the portion of $\partial\mathcal{B}$ with the normal along $+\hat{e}_1$ such that we have uniform $\Sigma_{31} = \Sigma_{13} = -\tau$ ($\tau > 0$) everywhere in the domain. This results in a dislocation driving force per unit volume $\boldsymbol{f} = f\hat{e}_2 = \tau b l' \hat{e}_2$, where l' has units m^{-2}. We assume that the dislocation instantaneously begins to move with a constant (subsonic) velocity $\boldsymbol{v} = v\hat{e}_2$ ($v = f/B^p > 0$); this is allowed because it satisfies the dissipation condition $\boldsymbol{f} \cdot \boldsymbol{v} > 0$. Note that for a straight screw dislocation moving at a constant velocity, the dislocation self-driving forces are not generated (Clifton and Markenscoff, 1981).

The motion of the dislocation will result in the evolution of $\boldsymbol{\alpha}^p = -\nabla \times (\boldsymbol{\alpha}^p \times \boldsymbol{v}^p)$ deduced from equation (3.27), which in turn will result in $\dot{\tilde{\boldsymbol{U}}}^p = \dot{\boldsymbol{U}}^p = \boldsymbol{\alpha}^p \times \boldsymbol{v}^p$ (the equality here is simply due to the single dislocation case) via equation (3.28). As can be deduced from equation (3.46), there will also be an evolution of the local stress field (a combination of the one induced by the dislocation and the traction boundary conditions), which will satisfy the static equilibrium condition derived from equation (3.34) at any instant in time. The dislocation motion will induce a change in the temperature field through the term $\boldsymbol{\sigma}:\boldsymbol{U}^p$ in equation (3.57); resulting in a heat flux given by equation (3.54). As a consequence, $\boldsymbol{\varepsilon}^\theta$ will evolve, specifically the components ε_{11}^θ, ε_{22}^θ and ε_{33}^θ. The combined effect of the traction-free boundary conditions along $\pm\hat{e}_2$ along with the evolutions of $\boldsymbol{\varepsilon}^\theta$ and $\boldsymbol{U}^p$, could result in the evolution of $\boldsymbol{\varepsilon}$, which could have an additional contribution to the evolution of θ as seen via in equation (3.57). The evolving θ would also contribute to the evolution of $\boldsymbol{\alpha}^p$ via the source term $\boldsymbol{S}^p$ seen in section 3.2 and entering equation (3.27); we shall assume that no other dislocation sources are present in $\mathcal{B}$. The spatially and temporally evolving θ could also result in the evolution of $\boldsymbol{\alpha}^\theta$ via equation (3.25b) to generate thermal quasi-dislocations. The combined effect of evolving $\boldsymbol{\alpha}^p$ and $\boldsymbol{\alpha}^\theta$ may or may not result in an evolution of $\boldsymbol{\alpha}$ via equation (3.29), and consequently, $\boldsymbol{U}^{e\perp}$, which would affect $\boldsymbol{\sigma}$ via equation (3.46). If we neglect body forces and the heat loss term ρr, and assume that all material properties remain constant, then the relevant set of field equations, initial conditions and boundary conditions to solve the current problem are:

Field Equations	Boundary conditions at any time t	Initial conditions
$\boldsymbol{\varepsilon}^\theta = \boldsymbol{\gamma}\Delta\theta$		
$\dot{\boldsymbol{\alpha}}^p = -\boldsymbol{\nabla} \times (\boldsymbol{\alpha}^p \times \boldsymbol{v}^p) + \boldsymbol{S}^p$		
$\dot{\boldsymbol{\varepsilon}}^p = \mathrm{sym}(\boldsymbol{\alpha}^p \times \boldsymbol{v}^p)$		
$\dot{\boldsymbol{\alpha}}^\theta = -\boldsymbol{\gamma} \cdot \left[\boldsymbol{\nabla}(\dot{\Delta}\theta) \cdot \mathbf{X}\right]$		
$\dot{\boldsymbol{\alpha}} = \dot{\boldsymbol{\alpha}}^\theta + \dot{\boldsymbol{\alpha}}^p$ and $\boldsymbol{\alpha} = \boldsymbol{\nabla} \times \boldsymbol{U}^{e\perp}$		
$\boldsymbol{\sigma} = \boldsymbol{C}:\left(\boldsymbol{\varepsilon} - \boldsymbol{\varepsilon}^p - \boldsymbol{\varepsilon}^\theta\right)$		
$\boldsymbol{\nabla} \cdot \boldsymbol{\sigma} = \mathbf{0}$		
$\boldsymbol{q} = -\boldsymbol{K} \cdot \boldsymbol{\nabla}\theta$		
$\boldsymbol{v}^p = v\hat{e}_2 = \tau b l'/B^p \hat{e}_2;\ v = constant$		
$\rho c_\varepsilon \dot{\theta} = \boldsymbol{\nabla} \cdot (\boldsymbol{K} \cdot \boldsymbol{\nabla}\theta) + \boldsymbol{\sigma}:\dot{\boldsymbol{\varepsilon}}^p - \theta\boldsymbol{\beta}:(\dot{\boldsymbol{\varepsilon}} - \dot{\boldsymbol{\varepsilon}}^p)$	$\boldsymbol{t} = \boldsymbol{\sigma} \cdot (\pm\hat{e}_2) = 0$, on $x_2 = \pm L$	$\theta(\boldsymbol{x}, 0) = \theta_0; \forall \boldsymbol{x} \in \mathcal{B}$
	$\boldsymbol{t} = \boldsymbol{\sigma} \cdot \hat{e}_1 = -\tau\hat{e}_3$, on $x_1 = H$	$\boldsymbol{U}^{p\parallel}(\boldsymbol{x}, 0) = \mathbf{0}; \forall \boldsymbol{x} \in \mathcal{B}$
	$\boldsymbol{u} = 0$, on $x_1 = -H$	$\boldsymbol{\alpha}^p = \alpha_{33}(\theta_0)\hat{e}_3 \otimes \hat{e}_3$
	$\theta = \theta_0$, on $x_1 = \pm H$	$= b_0 l_0' \hat{e}_3 \otimes \hat{e}_3$
	$\theta = \theta_0$, on $x_2 = \pm L$	average line position
	Periodic on $x_3 = \pm W$	at $(0,0,x_3)$

(4.13)

Our goal here is to find an analytical solution of the temperature field induced by the moving screw dislocation within $\mathcal{B}$ at a given instant in time. It is impractical to obtain this solution by directly attempting to solve the above set of field equations subjected to the given initial and boundary conditions; the complexities arise from (i) the temporal and spatial evolutions involved, which would require using both Laplace and Fourier transforms, along with (ii) the interdependency of the field variables and their evolutions. In order to solve this problem, we adopt a time stepping approach. We discretize time in short intervals, say Δt, and assume that the magnitudes of all the variables remain constant during each of these short intervals. We solve for the heat equation using the new position of the dislocation line that it would attain at the end of that time interval to obtain the new temperature field. Then, at the end of that time interval, the other evolving field variables are updated. For simplicity, we solve the problem using $\Delta\theta = \theta - \theta_0$ instead of θ.

During the first interval Δt, the dislocation moves from $(0,0)$ to the position $(0, v\Delta t)$. During this motion, in accordance with our assumptions to solve this problem, we assume that the dislocation source term $\boldsymbol{S}^p$ does not evolve. In essence, during a time interval Δt, we only account for the translation of the screw dislocation, i.e. $\dot{\boldsymbol{\alpha}}^p = -\boldsymbol{\nabla} \times (\boldsymbol{\alpha}^p \times \boldsymbol{v}^p)$ (obtained by neglecting $\boldsymbol{S}^p$ from equation (3.27)). This

equation reduces to $\dot{l}' = -v l'_{,2}$ which at the end of Δt yields $l' \equiv \hat{l}'(x_1, x_2 - v\Delta t)$ (Acharya, 2001). The new temperature field $\Delta\theta$ due to this motion can be obtained by solving the following 2D inhomogeneous heat equation with Dirichlet temperature boundary conditions:

$$\left.\begin{aligned} \rho c_\varepsilon \dot{\Delta\theta} = k\left(\Delta\theta_{,11} + \Delta\theta_{,22}\right) + \underbrace{\tau v b_0 \hat{l}'_0(x_1, x_2 - v\Delta t)}_{f_0(x_1, x_2, t)} \\ \Delta\theta(-H, x_2, t) = \Delta\theta(H, x_2, t) = 0 \\ \Delta\theta(x_1, -L, t) = \Delta\theta(x_1, L, t) = 0 \\ \Delta\theta(x_1, x_2, 0) = 0 \end{aligned}\right\} \tag{4.14}$$

The ensuing temperature field, $\theta_1(\boldsymbol{x})$, will be heterogeneous and it will induce changes to ε^θ_{11}, ε^θ_{22} and ε^θ_{33}. As discussed earlier in this section, these thermal strains may result in the generation of stresses σ_{11}, σ_{22} and σ_{33} varying along $\hat{e}_1$ and $\hat{e}_2$, thermal quasi-dislocations densities $\alpha^\theta_{13} = \varepsilon^\theta_{11,2}$, $\alpha^\theta_{23} = -\varepsilon^\theta_{22,1}$, $\alpha^\theta_{31} = -\varepsilon^\theta_{33,2}$ and $\alpha^\theta_{32} = -\varepsilon^\theta_{33,1}$, and non-zero $\dot{\varepsilon}_{11}$, $\dot{\varepsilon}_{22}$ and $\dot{\varepsilon}_{33}$ (in combination with the mechanical boundary conditions). Since the moving dislocation acts as a heat source, the highest temperature changes will be localized within the dislocation core. Therefore, we also need to update the magnitudes of b and l' from b_0 and l'_0 to b_1 and l'_1, respectively, such that they satisfy $\dot{\boldsymbol{\alpha}}^p = \boldsymbol{S}^p$ (equation (3.25a)). All of these changes, could result in the evolution of $\boldsymbol{\alpha}$ (equation (3.29)), $\boldsymbol{U}^{e\perp}$ (equation (3.14)) and the components of $\boldsymbol{\sigma}$ (equation (3.46)) associated with the presence of the dislocation.

After updating all these variables, for the next time interval Δt, we would have to solve $\rho c_\varepsilon \dot{\theta} = k\left(\theta_{,11} + \theta_{,22}\right) + \tau v b_1 \hat{l}'_1(x_1, x_2 - 2v\Delta t) + \theta_0(3\lambda + 2\mu)\gamma(\dot{\varepsilon}_{11} + \dot{\varepsilon}_{22} + \dot{\varepsilon}_{33})$ with the initial condition $\theta_1(\boldsymbol{x}) - \theta_0$ and the same boundary conditions as in equation (4.14) to obtain $\theta_2(\boldsymbol{x})$. Note that for simplicity, we have chosen θ_0 instead of θ in the thermomechanical coupling term on the right-hand side of the temperature rate equation. After updating the variables as discussed in the previous paragraph, the procedure is repeated for the subsequent time intervals.

The subsequent time intervals involve solving the same equation set after updating the variables. By induction, at the $(j+1)^{th}$ time increment, we need to solve for the following equation set:

$$\left.\begin{aligned} \rho c_\varepsilon \dot{\Delta\theta} = k\left(\Delta\theta_{,11} + \Delta\theta_{,22}\right) + \underbrace{\tau v b_j \hat{l}'_j(x_1, x_2 - (j+1)v\Delta t) + \theta_0(3\lambda + 2\mu)\gamma(\dot{\varepsilon}_{11} + \dot{\varepsilon}_{22} + \dot{\varepsilon}_{33})}_{f_{j+1}(x_1, x_2, t)} \\ \Delta\theta(-H, x_2, t) = \Delta\theta(H, x_2, t) = 0 \\ \Delta\theta(x_1, -L, t) = \Delta\theta(x_1, L, t) = 0 \\ \Delta\theta(x_1, x_2, 0) = \theta_j(x_1, x_2) - \theta_0 \end{aligned}\right\} \tag{4.15}$$

The solution to (4.14) can be obtained by additively splitting the solution into (i) a part that solves for the initial boundary value problem without $f_{j+1}(x_1, x_2, t)$ and (ii) another part that solves for the inhomogeneous heat equation (i.e. with $f_{j+1}(x_1, x_2, t)$) but with zero initial condition. One of the standard approaches to solve part (i) is to use separation of variables and solving the resulting eigenvalue problem with symmetric boundary conditions using the Fourier series approach (Strauss, 2008). Then the solution to part (ii) follows directly from part (i). For our problem, we obtain the following solution for $\Delta\theta_{j+1}$:

$$\Delta\theta_{j+1}(x_1, x_2, t) = \sum_{m=1}^{\infty}\sum_{n=1}^{\infty} A_{mn} \sin\left(\frac{m\pi x_1}{H}\right) \sin\left(\frac{n\pi x_2}{L}\right) \exp\left(-\frac{k}{\rho c_\varepsilon}\left[\frac{m^2\pi^2}{H^2} + \frac{n^2\pi^2}{L^2}\right] t\right) + \int_0^t \sum_{m=1}^{\infty}\sum_{n=1}^{\infty} B_{mn}(\tau) \sin\left(\frac{m\pi x_1}{H}\right) \sin\left(\frac{n\pi x_2}{L}\right) \exp\left(-\frac{k}{\rho c_\varepsilon}\left[\frac{m^2\pi^2}{H^2} + \frac{n^2\pi^2}{L^2}\right](t - \tau)\right) d\tau \tag{4.16}$$

with

$$A_{mn} = \frac{1}{HL}\int_{-L}^{L}\int_{-H}^{H} \sin\left(\frac{m\pi x_1}{H}\right)\sin\left(\frac{n\pi x_2}{L}\right)\left(\theta_j(x_1,x_2)-\theta_0\right)dx_1dx_2$$

and

$$B_{mn}(\tau) = \frac{1}{HL}\int_{-L}^{L}\int_{-H}^{H} \sin\left(\frac{m\pi x_1}{H}\right)\sin\left(\frac{n\pi x_2}{L}\right)\frac{f_{j+1}(x_1,x_2,\tau)}{\rho c_\varepsilon}dx_1dx_2$$

If we set $\theta_j(x_1,x_2)-\theta_0 = 0,\ \forall x_1,x_2 \in \mathcal{B}$ in equation (4.16), then we obtain the solution to the problem set (4.14).

The solution in equation set (4.16) can be compared with the existing solutions for temperature evolution due to dislocation motion (De Hosson et al., 2001; Eshelby and Pratt, 1956; Freudenthal and Weiner, 1956). Note that these works do no account for the role of rise in temperature on the magnitude of the Burgers and line vectors, and dislocation density (equation (3.25a)). While the solution procedure for updating the dislocation density (and other field variables) has not been presented here, it is nevertheless possible to do so using the field equations presented in equation set (4.13).

5. Summary and conclusions

In this work, a strong coupling between the field dislocations mechanics (FDM) model (Acharya, 2003, 2001) and the heat conduction problem is proposed to obtain the T-FDM (thermal-FDM) model. The main motivation for developing this model is to study dislocation interactions with other defects and dislocation structure evolution in heat-affected crystalline solids experiencing strong rapidly changing temperature gradients such as those occurring during an additive manufacturing process. However, the proposed model could be applied to study the dynamics of individual dislocations of any kind and/or their ensembles under any permissible combination of displacement, traction, temperature and heat flux boundary conditions; note that such applications will require appropriately accounting for the self-stress and self-driving forces of dislocations.

Similar to most continuum-based dislocation mechanics models, the T-FDM modeling framework is based on the main governing principles of RT (rational thermodynamics): local thermodynamic equilibrium and the classical Clausius-Kelvin-Planck formulation of the second law of thermodynamics applied on the entire system. The T-FDM model operates at the length scale where it is possible to isolate individual dislocations. At this length scale, the assumption of local thermodynamic equilibrium is found to be respected even during very high temperature rates such as those occurring during an additive manufacturing process; the equilibrium definition of temperature is sufficient for such applications.

Kinematic relationships involving the elastic and plastic distortion are inherited from the FDM model, which uses the Stokes-Helmholtz decomposition to uniquely separate these distortions into their respective compatible and incompatible parts. Importantly, the T-FDM model accounts for incompatible thermal strains and an associated areal density, which is related to the curl of the incompatible thermal strains. The symmetric thermal strain tensor is separated into two asymmetric tensors, one of which is compatible and the other incompatible; this separation is similar to the Stokes-Helmholtz decomposition of elastic and plastic distortions.

The kinematic problem is complemented with temperature dependent energetic (Cauchy stress and entropy) and dissipative (dislocation driving forces and heat flux) constitutive relationships derived from the global dissipation and local free energy considerations. Exploitation of the properties of the Stokes-Helmholtz decomposition within the global dissipation formulation naturally leads us to obtain temperature dependent crystallographic dislocation driving forces, which are similar to those obtained in the FDM model.

Analytical solutions to some illustrative problems are used to demonstrate some of the predictive capabilities of the model as well as understand the significance of incompatible thermal strains in generating incompatible stresses. In particular, an analytical solution to the temperature change induced by an

infinitely-long moving screw dislocation is computed under Dirichlet temperature boundary conditions. The T-FDM modeling framework allows to account for the change in its dislocation density due to temperature changes induced by its own motion, which is unprecedented.

Prospective work includes numerical implementation of this model to enable the study of dislocation dynamics under transient temperature changes such as those occurring during additive manufacturing, extending the geometrically linear T-FDM model to a finite strain framework and up-scaling the model to the length scale where polycrystalline plasticity models operate.

Acknowledgements: The author extends profound thanks to the anonymous reviewers for their very valuable comments that have enriched this work.

6. References

Acharya, A., 2011. Microcanonical Entropy and Mesoscale Dislocation Mechanics and Plasticity. J Elast 104, 23–44. https://doi.org/10.1007/s10659-011-9328-3

Acharya, A., 2004. Constitutive analysis of finite deformation field dislocation mechanics. Journal of the Mechanics and Physics of Solids 52, 301–316. https://doi.org/10.1016/S0022-5096(03)00093-0

Acharya, A., 2003. Driving forces and boundary conditions in continuum dislocation mechanics. Proceedings of the Royal Society of London. Series A: Mathematical, Physical and Engineering Sciences 459, 1343–1363. https://doi.org/10.1098/rspa.2002.1095

Acharya, A., 2001. A model of crystal plasticity based on the theory of continuously distributed dislocations. Journal of the Mechanics and Physics of Solids 49, 761–784. https://doi.org/10.1016/S0022-5096(00)00060-0

Acharya, A., Knops, R.J., Sivaloganathan, J., 2019. On the structure of linear dislocation field theory. Journal of the Mechanics and Physics of Solids 130, 216–244. https://doi.org/10.1016/j.jmps.2019.06.002

Acharya, A., Roy, A., 2006. Size Effects and Idealized Dislocation Microstructure at Small Scales: Predictions of a Phenomenological Model of Mesoscopic Field Dislocation Mechanics: Part I. Journal of the Physics and Mechanics of Solids 54, 1687–1710. https://doi.org/10.1016/j.jmps.2006.01.009

Acharya, A., Tartar, L., 2011. On an equation from the theory of field dislocation mechanics. Bolletino dell Unione Matematica Italiana 4, 409–444.

Berbenni, S., Taupin, V., Djaka, K.S., Fressengeas, C., 2014. A Numerical Spectral Approach for Solving Elasto-Static Field Dislocation and G-Disclination Mechanics. International Journal of Solids and Structures.

Bilby, B.A., Bullough, R., Smith, E., 1955. Continuous Distributions of Dislocations: A new Application of the Methods of Non-Riemannian Geometry. Proceedings of the Royal Society of London: Series A, Mathematical and physical sciences 231, 263–273.

Clifton, R.J., Markenscoff, X., 1981. Elastic precursor decay and radiation from nonuniformly moving dislocations. Journal of the Mechanics and Physics of Solids 29, 227–251. https://doi.org/10.1016/0022-5096(81)90028-4

Coleman, B.D., 1964. Thermodynamics of materials with memory. Arch. Rational Mech. Anal. 17, 1–46. https://doi.org/10.1007/BF00283864

Coleman, B.D., Gurtin, M.E., 1967. Thermodynamics with Internal State Variables. J. Chem. Phys. 47, 597–613. https://doi.org/10.1063/1.1711937

Coleman, B.D., Mizel, V.J., 1963. Thermodynamics and departures from Fourier's law of heat conduction. Arch. Rational Mech. Anal. 13, 245–261. https://doi.org/10.1007/BF01262695

Coleman, B.D., Noll, W., 1960. An approximation theorem for functionals, with applications in continuum mechanics. Arch. Rational Mech. Anal. 6, 355–370. https://doi.org/10.1007/BF00276168

Coleman, B.D., Owen, D.R., 1975. On thermodynamics and elastic-plastic materials. Arch. Rational Mech. Anal. 59, 25–51. https://doi.org/10.1007/BF00281515
Coleman, B.D., Owen, D.R., 1974. A mathematical foundation for thermodynamics. Arch. Rational Mech. Anal. 54, 1–104. https://doi.org/10.1007/BF00251256
Coleman, B.D., Owen, D.R., Serrin, J., 1981. The second law of thermodynamics for systems with approximate cycles. Arch. Rational Mech. Anal. 77, 103–142. https://doi.org/10.1007/BF00250620
De Hosson, J.T.M., Roos, A., Metselaar, E.D., 2001. Temperature rise due to fast-moving dislocations. Philosophical Magazine A 81, 1099–1120. https://doi.org/10.1080/01418610108214431
Eshelby, J.D., 1957. The determination of the elastic field of an ellipsoidal inclusion, and related problems. Proceedings of the Royal Society of London. Series A. Mathematical and Physical Sciences 241, 376–396. https://doi.org/10.1098/rspa.1957.0133
Eshelby, J.D., Pratt, P.L., 1956. Note on the heating effect of moving dislocations. Acta Metallurgica 4, 560–562. https://doi.org/10.1016/0001-6160(56)90056-6
Forest, S., 2008. Some links between Cosserat, strain gradient crystal plasticity and the statistical theory of dislocations. Philosophical Magazine 88, 3549–3563.
Fox, N., 1966. A Continuum Theory of Dislocations for Single Crystals. IMA J Appl Math 2, 285–298. https://doi.org/10.1093/imamat/2.4.285
Freudenthal, A.M., Weiner, J.H., 1956. On the Thermal Aspect of Fatigue. Journal of Applied Physics 27, 44–50. https://doi.org/10.1063/1.1722194
Ghoniem, N.M., Tong, S.-H., Sun, L.Z., 2000. Parametric dislocation dynamics: A thermodynamics-based approach to investigations of mesoscopic plastic deformation. Phys. Rev. B 61, 913–927. https://doi.org/10.1103/PhysRevB.61.913
Gurtin, M.E., 2002. A gradient theory of single-crystal viscoplasticity that accounts for geometrically necessary dislocations. Journal of the Mechanics and Physics of Solids 50, 5–32. https://doi.org/10.1016/S0022-5096(01)00104-1
Gurtin, M.E., 2000. On the plasticity of single crystals: free energy, microforces, plastic-strain gradients. Journal of the Mechanics and Physics of Solids 48, 989–1036. https://doi.org/10.1016/S0022-5096(99)00059-9
Gurtin, M.E., 1968. On the thermodynamics of materials with memory. Arch. Rational Mech. Anal. 28, 40–50. https://doi.org/10.1007/BF00281562
Kosevich, A.M., 1979. Crystal dislocations and the theory of elasticity, in: Dislocations in Solids, Nabarro, F. R. N. (Editor). North Holland Publishing Company, Amsterdam, pp. 33–141.
Kratochvil, J., Dillon, O.W., 1969. Thermodynamics of Elastic-Plastic Materials as a Theory with Internal State Variables. Journal of Applied Physics 40, 3207–3218. https://doi.org/10.1063/1.1658167
Kröner, E., 1981. Continuum theory of defects, in: Physics of Defects. North-Holland Publ. Co., Amsterdam, pp. 217–315.
Kröner, E., 1959. Allgemeine Kontinuumstheorie der Versetzungen und Eigenspannungen. Arch. Rational Mech. Anal. 4, 273–334. https://doi.org/10.1007/BF00281393
Kröner, E., 1958. Kontinuumstheorie der versetzungen und eigenspannungen. Ergebnisse der Angewandten Mathematik 5, 1–179.
Lebon, G., Jou, D., Casas-Vázquez, J., 2008. Understanding Non-equilibrium Thermodynamics: Foundations, Applications, Frontiers. Springer-Verlag, Berlin Heidelberg. https://doi.org/10.1007/978-3-540-74252-4
Maitournam, H., 2017. Matériaux et structures anélastiques. Les éditions de l'Ecole polytechnique, Palaiseau, France.
Meixner, J., 1973. The entropy problem in thermodynamics of processes. Rheol Acta 12, 465–467. https://doi.org/10.1007/BF01503000
Mura, T., 1963. Continuous Distribution of Moving Dislocations. Philosophical Magazine 8, 843–857.
Nye, J.F., 1953. Some geometrical relations in dislocated crystals. Acta Metallurgica 1, 153–162. https://doi.org/10.1016/0001-6160(53)90054-6

Olmsted, D.L., HectorJr, L.G., Curtin, W.A., Clifton, R.J., 2005. Atomistic simulations of dislocation mobility in Al, Ni and Al/Mg alloys. Modelling Simul. Mater. Sci. Eng. 13, 371–388. https://doi.org/10.1088/0965-0393/13/3/007

Roy, A., Acharya, A., 2006. Size Effects and Idealized Dislocation Microstructure at Small Scales: Predictions of a Phenomenological Model of Mesoscopic Field Dislocation Mechanics: Part II. Journal of the Physics and Mechanics of Solids 54, 1711–1743. https://doi.org/10.1016/j.jmps.2006.01.012

Salencon, J., 2001. Handbook of Continuum Mechanics: General Concepts Thermoelasticity. Springer-Verlag, Berlin Heidelberg. https://doi.org/10.1007/978-3-642-56542-7

Serrin, J., 1979. Conceptual analysis of the classical second laws of thermodynamics. Arch. Rational Mech. Anal. 70, 355–371. https://doi.org/10.1007/BF00281160

Strauss, W.A., 2008. Partial Differential Equations: An Introduction, 2nd ed. John Wiley and Sons, Inc., Hoboken, New Jersey, USA.

Truesdell, C., 1984. Rational Thermodynamics, 2nd ed. Springer-Verlag, New York. https://doi.org/10.1007/978-1-4612-5206-1

Truesdell, C., 1968. Thermodynamics for Beginners, in: Parkus, H., Sedov, L.I. (Eds.), Irreversible Aspects of Continuum Mechanics and Transfer of Physical Characteristics in Moving Fluids, IUTAM Symposia. Springer, Vienna, pp. 373–389. https://doi.org/10.1007/978-3-7091-5581-3_26

Truesdell, C., Noll, W., 2004. The Non-Linear Field Theories of Mechanics, 3rd ed. Springer-Verlag, Berlin Heidelberg. https://doi.org/10.1007/978-3-662-10388-3

Truesdell, C., Toupin, R., 1960. The Classical Field Theories, in: Flügge, S. (Ed.), Principles of Classical Mechanics and Field Theory / Prinzipien Der Klassischen Mechanik Und Feldtheorie, Encyclopedia of Physics / Handbuch Der Physik. Springer Berlin Heidelberg, Berlin, Heidelberg, pp. 226–858. https://doi.org/10.1007/978-3-642-45943-6_2

Upadhyay, M.V., Capolungo, L., Taupin, V., Fressengeas, C., 2013. Elastic constitutive laws for incompatible crystalline media: the contributions of dislocations, disclinations and G-disclinations. Philosophical Magazine 93, 794–832. https://doi.org/10.1080/14786435.2012.733829

Willis, J.R., 1967. Second-order effects of dislocations in anisotropic crystals. International Journal of Engineering Science 5, 171–190. https://doi.org/10.1016/0020-7225(67)90003-1

Zhang, X., Acharya, A., Walkington, N.J., Bielak, J., 2015. A single theory for some quasi-static, supersonic, atomic, and tectonic scale applications of dislocations. Journal of the Mechanics and Physics of Solids 84, 145–195. https://doi.org/10.1016/j.jmps.2015.07.004

Zhu, Y., Chapman, S.J., Acharya, A., 2013. Dislocation motion and instability. Journal of the Mechanics and Physics of Solids 61, 1835–1853. https://doi.org/10.1016/j.jmps.2013.03.002